sciendo

ACV with/without IVM: a new talk on intestinal CDX2 and muscular CD34 and Cyclin D1 during *Trichinella spiralis* infection

E. A. EL SAFTAWY[1,2], B. E. ABOULHODA[3], F. E. HASSAN[4,5], M. A. M. ISMAIL[1], M. A. ALGHAMDI[6,7], S. M. HUSSEIN[3], N. M. AMIN[1,*]

[1]Medical Parasitology Department, Faculty of Medicine, Cairo University, Cairo, Egypt,
*E-mail: *nmabdelrazek@kasralainy.edu.eg* or *noha_212@cu.edu.eg*; [2]Medical Parasitology Department, Armed Forces
College of Medicine, Cairo, Egypt; [3]Department of Anatomy and Embryology, Faculty of Medicine, Cairo University, Cairo, Egypt;
[4]Medical Physiology Department, Kasr Alainy, Faculty of Medicine, Cairo University, Giza 11562, Egypt; [5]General Medicine Practice
Program, Department of Physiology, Batterjee Medical College, Jeddah 21442,Saudi Arabia; [6]College of Medicine, King Khalid
University, Abha 62529, Saudi Arabia; [7]Genomics and Personalized Medicine Unit, College of Medicine, King Khalid University,
Abha 62529, Saudi Arabia

Article info

Summary

The current study assessed the efficacy of Acyclovir (ACV) and Ivermectin (IVM) as monotherapies and combined treatments for intestinal and muscular stages of *Trichinella* spiralis infection. One-hundred Swiss albino mice received orally 250 ± 50 infectious larvae and were divided into infected-untreated (Group-1), IVM-treated (Group-2), ACV-treated (Group-3), combined IVM+ACV (Group-4), and healthy controls (Group-5). Each group was subdivided into subgroup-A-enteric phase (10 mice, sacrificed day-7 p.i.) and subgroup-B-muscular phase (10 mice, sacrificed day-35 p.i.). Survival rate and body weight were recorded. Parasite burden and intestinal histopathology were assessed. In addition, immunohistochemical expression of epithelial CDX2 in the intestinal phase and CyclinD1 as well as CD34 in the muscular phase were evaluated. Compared, IVM and ACV monotherapies showed insignificant differences in the amelioration of enteric histopathology, except for lymphocytic counts. In the muscle phase, monotherapies showed variable disruptions in the encapsulated larvae. Compared with monotherapies, the combined treatment performed relatively better improvement of intestinal inflammation and reduction in the enteric and muscular parasite burden. CDX2 and CyclinD1 positively correlated with intestinal inflammation and parasite burden, while CD34 showed a negative correlation. CDX2 positively correlated with CyclinD1. CD34 negatively correlated with CDX2 and CyclinD1. IVM +ACV significantly ameliorated CDX2, CyclinD1, and CD34 expressions compared with monotherapies. Conclusion. *T. spiralis* infection-associated inflammation induced CDX2 and CyclinD1 expressions, whereas CD34 was reduced. The molecular tumorigenic effect of the nematode remains questionable. Nevertheless, IVM +ACV appeared to be a promising anthelminthic anti-inflammatory combination that, in parallel, rectified CDX2, CyclinD1, and CD34 expressions.

Keywords: *T. spiralis*; Ivermectin; Acyclovir; Inflammation; CDX2; CyclinD1; CD34

Introduction

Trichinella spiralis infection is a serious global foodborne zoonosis in humans and other mammals (CDC, 2023). It is caused by ingesting undercooked porcine products, which has been seriously associated with outbreaks (Dubinský *et al*., 2016). The global incidence of trichinellosis is challenging to estimate. In China, for instance, more than 40 million persons are at risk of infection (Bai *et al*., 2017).

---

* – corresponding author

Following ingestion of the infective larvae, it establishes a distinctive intracellular niche in the mucosal epithelium (between the epithelia and its basal lamina). Larvae then molt to adult worms within 2 – 5 days. After that, the adult worm mates in the non-membrane-bound portion of the enteric columnar epithelium. The fertilized females burrow deep into the cytosol of cells of the enteric mucosa and probably the absorptive and goblet cells and discharge newborn larvae in the blood circulation (5 to 15 days post-infection) (CDC, 2023).

The new generation of larvae (L1) enters the skeletal muscle cells to establish their niches, "the nurse cells," and increase in size from 100 to 1000 µm, i.e., ten times. Literally, the infected muscle cell becomes dominated by the parasite to serve the nourishment and protection of the larvae. The development of nurse cells is associated with multiple cellular alterations and the construction of a host-derived collagen capsule. Skeletal muscles have been recognized as a unique site for the formation of nurse cells (Despommier, 1998). However, the molecular processes governing these intricate cellular alterations are largely unknown, and there are few protein markers for inducing the infected-cell phenotype (Beiting *et al*., 2006).

Proposing a parasite-host interface will stimulate the development of novel anthelmintic strategies and provide a better understanding of how parasite's strategies adjust while establishing infection at the host. For example, CDX2 expression in the intestine, a crucial transcription factor related to the caudal-related homeobox gene family with a specific expression pattern, plays a vital role in intestinal homeostasis and mucosal immunity. Physiologically, CDX2 affords the stem cells with the information that maintains the proliferation of the mucosal epithelium, the differentiation of the normal phenotype, the regulation of the cell cycle, cellular adhesion, and nutrition (Freund *et al*., 2015; Wang *et al*., 2005).

In the muscles, Cyclin D1 is a physiologically critical protein that encodes the regulatory subunit of a holoenzyme that phosphorylates and deactivates the retinoblastoma protein and accelerates cell cycle progression through the G1-S phase (Mademtzoglou & Relaix, 2022). CD34 is a transmembrane sialomucin receptor biomarker and an indicator for hematopoietic progenitors and stem cells. Yet, expression of CD34 occurs in various cell types, for example, the interstitial dendritic cells, the epithelial progenitors, and the vascular endothelial progenitor cells (Alfaro *et al*., 2011; Kong *et al*., 2016). CD34 also acts as a cell-to-cell adhesion factor. In recent years, skeletal muscle satellite cells, myogenic progenitors, have been demarcated relying upon the expression of CD34. Therefore, several authors explored CD34 to regenerate injured muscle cells (Kapoor *et al*., 2020; Mañas-García *et al*., 2020; Wolcott & Woodard, 2020). However, the expression of CDX2, Cyclin D1, and CD34 after being challenged with *T. spiralis* infection has not been investigated.

Another point is the pharmacology-host-parasite interface, where albendazole, the classic therapy, has been criticized for its poor activity against encysted *T. spiralis* larvae in the muscle phase (Siriyasatien *et al*., 2003). Also, Benzimidazoles have been determined by their limited bioavailability and increasing drug resistance (Gottstein *et al*., 2009). Instead, Ivermectin (IVM) was identified as a reference treatment for trichinosis by (Basyoni & El-Sabaa, 2013). We hypothesize that *T. spiralis* resides inside the host's cells to establish its nest, making it challenging to propose an efficient and safe therapy. Also, it is difficult to intend therapy that would hamper the parasite without detrimental effects on the host's cells. Interestingly, *T. spiralis* was regarded as a non-replicating- virus-like intracellular organism that can play a role in modulating the genomic material of the host to attain well-developed nurse cells (Despommier, 1990) successfully. In this context, we inquired if Acyclovir (ACV), one of the most common antiviral drugs (mainly the Herpes family), can be "repurposed" to be used against *T. spiralis* as well (Schalkwijk *et al*., 2022). ACV is a guanine nucleoside analog at which the presence of viral thymidine kinase enzyme determines its activation into ACV triphosphate. In turn, activated ACV acts as a competitive inhibitor of the viral DNA polymerase enzyme and a chain terminator in the synthesis of the viral DNA, therefore hampering the virus (Lefaan *et al*., 2022). Interestingly, thymidine kinases were highly detected in *T. spiralis* in both adult and larva stages (Wińska *et al*., 2005). Additionally, it is present in the cytosol of mammalian cells (Frisk *et al*., 2020); thus, it may act on the parasitized host cells.

Based on the data above and hypothesis, the current study was to assess the histopathological changes in the intestine and muscle phases following infection with *T. spiralis*, show the expression of the host-derived CDX2 in the intestine and Cyclin D1 and CD34 in the muscle following *T. spiralis* infection, and investigate the potential effect of ACV with or without IVM on the intestinal CDX2 and muscular Cyclin D1 and CD34 in relation to the parasite load and histological changes.

Material and Methods

Experimental animals
One hundred Swiss albino male mice were employed in the current research. Involved animals were pathogen-free, laboratory-bred, weighing 25 ± 5 g, and were purchased via the Theodor Bilharz Research Institute (TBRI), Cairo, Egypt. The mice were set on a standard diet, humidity, and housing conditions with a temperature of 24 °C. The study was approved by the reviewers of the ethical committee of the Institutional Animal Care and Use Committee (CU-IACUC) (0334) at Cairo University with approval number CU-III-F-74-22. It was performed in agreement with the international ethical guidelines.

Experimental design
The mice were divided into five major groups (Group 1 – 5), each involving 30 mice; 15 mice were determined for the intestinal phase to be sacrificed on day 7 p.i. (subgroup A), while the other 15 animals were designated for the muscular phase and were sac-
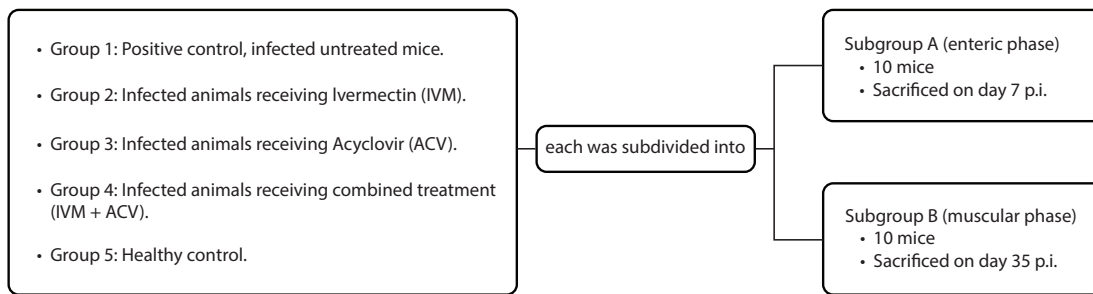
Fig. 1. Experimental design.

rificed on day 35 p.i. (subgroup B). Nevertheless, an equal number of mice (n = 10) was blindly selected per subgroup to avoid statistical bias due to the variant mortality rates to accomplish further assessments (Fig. 1).

Experimental infection

Each mouse received 250 ± 50 infectious *T. spiralis* larvae (Instituto Superiore di Sanit'a code or ISS number: ISS6158), which were originally purchased from the Cairo abattoir and maintained in subsequent cycles using BALB/c mice at the TBRI according to Gamble (1996). In brief, dissected muscles from infected slaughtered mice were treated for two hours at 37 °C in distilled water with 1 % HCl and 1 % pepsin. An electric stirrer was used to whisk the mixture sporadically while incubating. The digested material was filtered on a 50 mm mesh to eliminate bulky particles. The infectious larvae were then gathered on a screen (200 mm mesh), washed twice, and then suspended in a cylindrical container with 150 ml of tap water. The larval suspension was allowed to settle, and its supernatant was eliminated. Using dissecting microscopy, larvae were retrieved and quantified to determine each animal's precise infectious dosage (Franssen *et al*., 2011).

Drug administration

IVM (Iverzine 6 mg tablets, Uni Pharma, Egypt) and ACV (Acyclovir 200 mg tablets, Memphis, Egypt) were dissolved in distilled water. Referring to Paget and Barnes (1964), doses were estimated by renovating the therapeutic human doses to doses for animals. IVM was orally administered on days 1 and 5 p.i. for the intestinal phase (subgroup A) and on days 15 and 30 p.i. for the muscular phase (subgroup B) at a dose of 4 µg /mouse/day (Basyoni and El-Sabaa, 2013). Also, oral ACV was given at a dose of 10 mg/kg/day for 7 days in subgroup A (starting from day 1 p.i.) and in subgroup B (starting from day 28 p.i.) for, respectively, the intestinal and muscular phases (Quenelle *et al*., 2018).

Survival analysis and weight gain (g)

In the four groups of mice receiving the current protocol of infection and treatment, survival rate and body weight in grams (g) were detected versus their healthy control every day for the initial 7 days p.i. in subgroup A and at the end of the study period, i.e., day 35

p.i. in subgroups B.

Animal sacrifice

To assess the impact of the current therapeutic protocols on adults and larvae, animals were respectively sacrificed under anesthesia by cervical dislocation 7 days p.i. for the intestinal phase (subgroups A) and 35 days p.i. for the muscular phase (subgroups B) (Pan *et al*., 2023).

Parasitological examination

Quantification of adults in the enteric fluid

On day 7 p.i., the number of mature helminths per milliliter of intestinal fluid was microscopically identified. The procedure involved slicing the small intestines into small fragments after being longitudinally opened and saline. After 2 hours of incubation of the specimens in PBS at 37 °C, the adult parasites were gathered and enumerated using dissecting microscopy.

Histological assessment and quantification of adults and larvae in tissues

On days 7 and 35, after infection and therapeutic challenge, the small intestine and muscles were successively obtained from infected animals and fixed for 24 h in 4 % formalin. Then, tissues were embedded in paraffin, and cut sections of 3-µm-thickness sections were stained for histological examination using the routine H and E stain. Intestinal sections of each group were assessed for the architecture of the infected villi: villus (V) length/crypt (C) depth, counts of goblet cells/villus, counts of crypts/villus, counts of Paneth cells/crypt, and counts of inflammatory infiltrates/villus. The assessment was done in 20 villi/mouse, and mean values were calculated. The larvae, the nursing cells, and the surrounding capsule were investigated in the muscle cut sections. Average scoring of the muscular changes was done for each group in 10 larvae (randomly selected)/mouse regarding (1) larvae structures: intact-altered, (2) capsule inflammatory infiltrates: mild-moderate-intense, and (3) nurse cell: intact-altered. Adults in intestinal cut-sections were enumerated per 100 villi; also, the encapsulated larvae on muscle sections were enumerated per low power field (40×) using the gridding method (El Saftawy *et al*., 2020; Helal *et al*., 1991). The pathological evaluation was done by two pathologists in two different settings using a Zeiss microscope (Zeiss, Germany) and morphocytometry.

Table 1. Means of body weight and survival rate in all experimental subgroups.

	Group 1 (infected - untreated)		Group 2 (IVM treated)		Group 3 (ACV treated)		Group 4 (combined treatment)		Group 5 (healthy)		P-value
	M°	SD	M°	SD	M°	SD	M°	SD	M°	SD	
Body weight (g) at day 7 p.i. (subgroups, A)	15.70[a]	1.64	22.90[b]	2.13	23.10[b]	2.23	26.20[c]	1.03	26.60[c]	1.43	< 0.001
Body weight (g) at day 35 p.i. (subgroups, B)	18.20[a]	2.20	22.30[b]	2.11	23.70[b]	2.41	27.00[c]	1.25	27.30[c]	1.64	< 0.001
Survival rate	11[a]	73.3%	12[a,b]	80.0%	12[a,b]	80.0%	14[a,b]	93.3%	15[b]	100.0%	

g – grams; M° – mean; in the superscripts – similar letters, p-value >0.05, while different letters p-value < 0.05.

Immunohistochemical examination

For immunological staining, paraffin sections from all study groups' small intestine and muscles were prepared on adhesive-coated glass slides. Hydrogen peroxide 3 % was used to hamper endogenous peroxide after being de-waxed and rehydrated. Slides were placed in a thermostatic bath filled with preheated ethylene diamine tetra acetic acid (EDTA) for 30 minutes at 98 °C in order to retrieve the antigens. Thereafter, cooling down was done for 20 minutes at ambient temperature. The slides containing intestinal specimens were incubated with the anti-CDX2 antibody [EPR2764Y] (#ab76541). However, muscle specimens were incubated with the monoclonal antibodies anti-Cyclin D1 antibody - C-terminal (#ab185241) and anti-CD34 antibody [EP373Y] (#ab81289). Meyer's hematoxylin was utilized as a counterstain after the diaminobenzidine (DAB) reaction to visualize the antigen-antibody combination. In the negative control, the primary antibody was omitted. A brown stain determined the positive immune reaction; as long it is not an artifact or a background (El Saftawy *et al*., 2020; Helal *et al*., 1991).

Image analysis by real-time quantitative morpho-cytometry

The pathological and morphometric analysis was carried out using a Leica Qwin 500 Image Analyzer (LEICA Imaging Systems Ltd., Cambridge, England). Optical density (OD) was automatically measured in ten fields, and quantitative values were saved for further statistical analysis (El Saftawy *et al*., 2020).

Statistical analysis of collected data

Data were coded and entered using the statistical package for the Social Sciences (SPSS) version 28 (IBM Corp., Armonk, NY, USA). Data was summarized using mean and standard deviation for quantitative variables and frequencies (number of cases) and relative frequencies (percentages) for categorical variables. Comparisons between groups were done using analysis of variance (ANOVA) with multiple comparisons post hoc test in normally distributed quantitative variables while non-parametric Kruskal-Wallis test and Mann-Whitney test were used for non-normally distributed quantitative variables (Chan, 2003a). A chi-square (c2) test was performed to compare categorical data. An exact test was used when the expected frequency was less than 5 (Chan, 2003b). Correlations between quantitative variables were done using the Spearman correlation coefficient (Chan, 2003c). P-values less than 0.05 were considered statistically significant.

Ethical Approval and/or Informed Consent

The study was approved by the Institutional Animal Care and Use Committee (CU-IACUC), Faculty of Sciences, Cairo University (CU: III-F-74-22). All procedures of the current experiment and study were in accordance with international guidelines for the use of laboratory animals.

Table 2. Counts of *Trichinella spiralis* adult worms in enteric fluid and intestinal tissue on day 7 p.i.

	Subgroup 1A (infected untreated)		Subgroup 2A (IVM treated)			Subgroup 3 A (ACV treated)			Subgroup 4A (combined treatment)			Subgroup 5A (healthy)		P-value
	M°	SD	M°	SD	R%	M°	SD	R%	M°	SD	R%	M°	SD	
No. of adults / milliliter	173.2[a]	65	46.2[b]	8.57	73.3%	45.6[b]	10.25	73.7%	21.7[b]	8.82	87.5%	NA	.	< 0.001
No. of adults / 100 villi	30.1[a]	14	12[b]	5.08	60.1%	10.10[b,c]	3.93	66.5%	1.8[c]	1.32	94.02%	NA	.	< 0.001

No. – number; M° – mean; R% – reduction rate; NA – not applicable, in the superscripts – similar letters, p-value > 0.05 while different letters p-value < 0.05.

Table 3. Intestinal histopathological changes on day 7 p.i. (acute stage).

	Subgroup 1A (infected untreated)		Subgroup 2A (IVM treated)		Subgroup 3 A (ACV treated)		Subgroup4 A (combined treatment)		Subgroup 5A (healthy)		P-value
	M°	SD	M°	SD	M°	SD	M°	SD	M°	SD	
V length /C depth ratio	1.39[a]	0.24	5.07[b]	0.80	4.87[b]	0.93	5.07[b]	0.80	5.60[b]	1.07	< 0.001
lymphocyte counts/villus	110.00[a]	13.03	50.20[b]	8.35	18.80[c]	4.26	6.60[d]	1.78	6.50[d]	1.84	< 0.001
Goblet cell counts /villus	45.50[a]	5.02	12.40[b]	2.27	12.40[b]	2.32	10.70 [b,c]	1.57	8.60[c]	0.97	< 0.001
No. of Paneth cells/crypt	16.90[a]	2.18	6.60[b]	0.97	6.00[b]	0.82	5.70[b]	0.82	5.70[b]	1.49	< 0.001
No. of crypts /villus	8.30[a]	1.89	2.30[b]	0.82	2.40[b]	0.70	1.60[b]	0.70	1.50[b]	0.53	< 0.001

No. – number; M° – mean; V – villus; C – crypt; in the superscripts – similar letters, p-value > 0.05, while different letters p-value < 0.05.

Results

Survival rate and body weight

The overall survival rate of mice showed insignificant differences between groups, with a p-value of 0.213. Yet, in the combined treatment (IVM + ACV), the survival rate was 93.3 %, while in the infected untreated mice, it was 73.3 %. Healthy control had a survival rate of 100 %. The mean weight in grams in all treated groups versus infected untreated animals was p-value ≤ 0.001 at either day 7 p.i. or day 35 p.i.. Further details concerning body weight are illustrated in Table 1.

Histopathological examination

Intestinal phase of *T. spiralis* infection (Day 7 p.i., acute stage)
Burden of T. spiralis adult worms

As shown in Table 2, the burden of adult worms in the intestinal tissues at day 7 p.i. was determined as the number of adults/ ml of enteric fluid and the number of adults/100 villi. The mean adult count in infected untreated animals (subgroup1A) was estimated to be approximately 173 ± 65/ml and 30 ± 14.02/100 villi (p-value < 0.001). Comparing treated Subgroups, the number of adults/ml in Subgroup 2A versus Subgroup 3A, Subgroup 2A versus Subgroup 4A, and Subgroup 3A versus Subgroup 4A were of p-values 1,
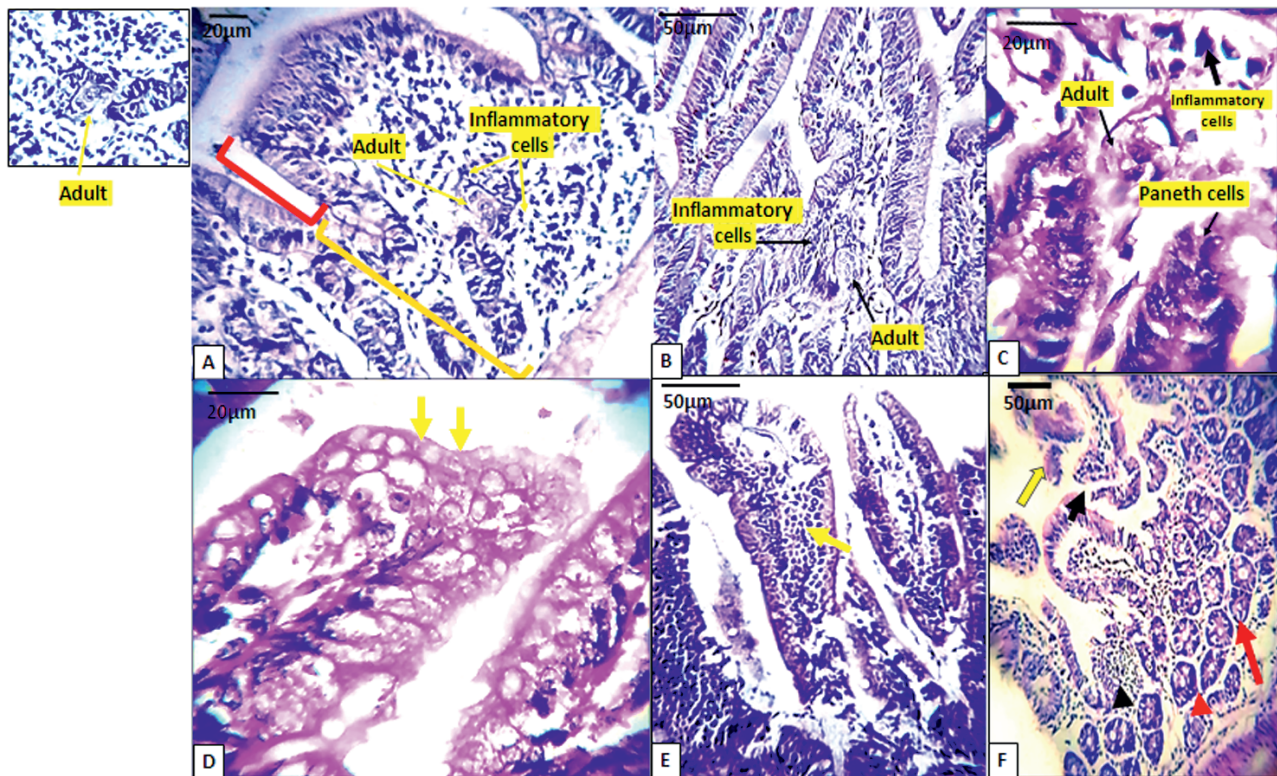
Fig. 2. Photomicrographs of H&E-stained small intestine in infected and untreated mice at day 7p.i.. A, B, & C show adults' cut sections invading the core and base of the intestinal villi in three different tissue cut sections surrounded with dense inflammatory infiltrates. Yet, (A) shows a reduced V length/C depth ratio, flattening villi, and shedding of epithelial cells (C) shows increased Paneth cells with eosinophilic cytoplasm, (D) shows hyperplasia of goblet cells, (E) shows increased inflammatory cells in the neighboring villi, (F) shows flattening and hyperplasia of the crypts of the villi (red arrow), disrupted villi (yellow arrow), and dense inflammatory cells (black arrows).
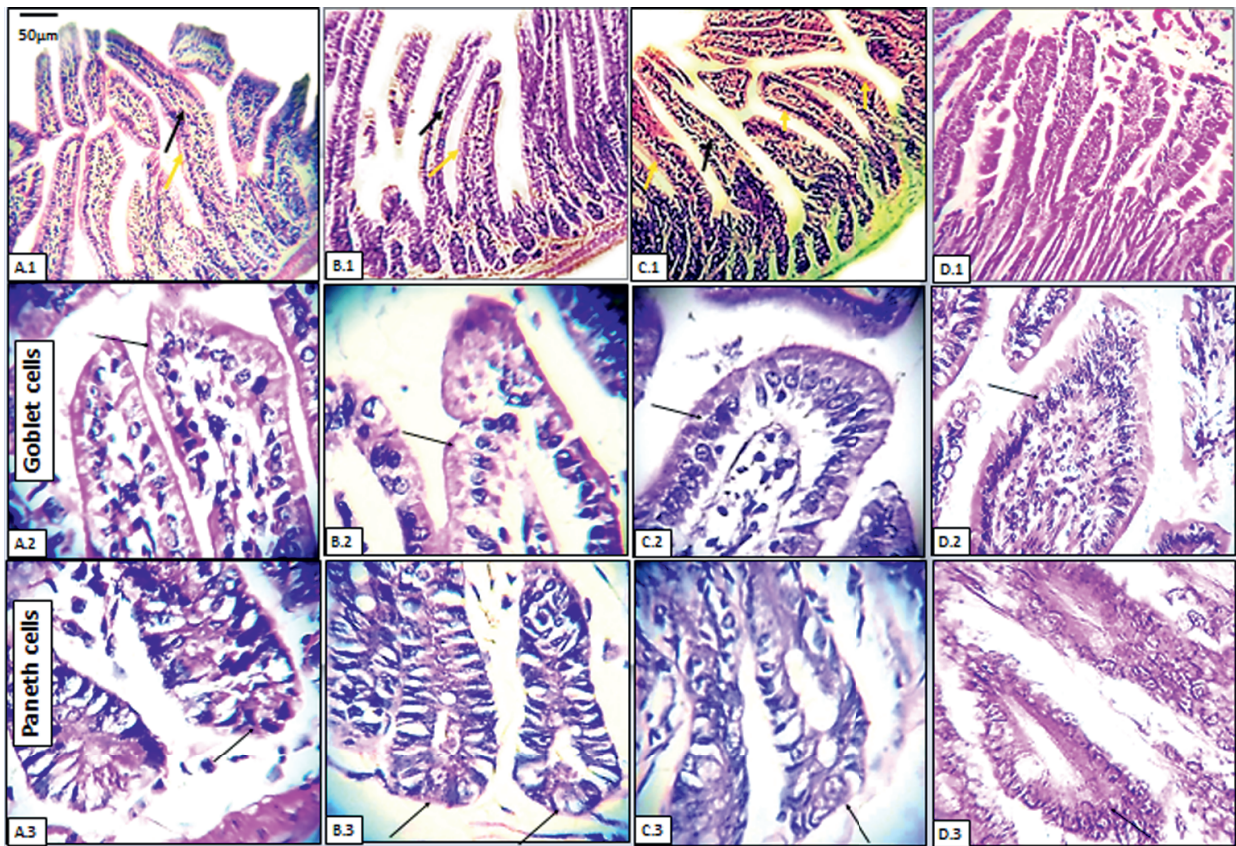
Fig. 3. Photomicrographs of H&E -stained small intestine in infected and treated mice at day 7 p.i.. (A.1) IVM treated mice, showing finger-like villi with apparently intact epithelial lining (yellow arrow), moderate inflammatory infiltrates (black arrow), and few disruptions in the surface of the villi. (A.2 and A.3) show goblet and Paneth cells respectively (black arrows). (B.1) ACV-treated mice, showing relatively intact epithelium lining with scarce disruption and reduced inflammatory infiltrates in finger-like villi (black arrows). (B.2 and B.3) show goblet and Paneth cells respectively (black arrows). (C.1) Combined treatment (IVM+ACV) showing finger-like and tongue-like villi with a mild intensity of the inflammatory infiltrate (black arrow), intact epithelium lining (yellow arrow). (C.2 and C.3) show few discrete goblets and Paneth cells respectively (black arrows). (D) Healthy control.

0.663, and 0.715 respectively. Also, the number of adults/100 villi in Subgroup 2A versus Subgroup 3A, Subgroup 2A versus Subgroup 4A, and Subgroup 3A versus Subgroup 4A showed p-values 1, 0.034, and 0.131 respectively. Further details are presented in Table 2.

Intestinal histopathological changes
The V length /C depth ratios in IVM and ACV, either as monotherapies or in combination, were restored versus infected untreated mice with p-value < 0.001. However, the V length /C depth ratio amelioration was more pronounced in the combined treatment (5.07 ± 0.8). Overall, treated groups and healthy controls showed insignificant differences in the V length /C depth ratios (p-value ≥ 0.05). Concerning lymphocyte counts/villus, the villi of the infected untreated animals versus treated and healthy mice exhibited a marked increase in the lymphocytic counts (p-value < 0.001). In comparison, IVM, ACV, and combined treatment scored significant reductions in lymphocytic counts with p-values ≤ 0.05. Combined treatment and healthy mice were of insignificant difference (p-value = 1).

Regarding goblet cell counts/villus, treated groups showed p-values < 0.001 compared with infected untreated animals. Treated groups were of insignificant differences (p-value = 1). Nevertheless, only combined treatment versus healthy mice showed p-value = 1.

Counts Paneth cells/crypt and likewise the counts of crypts/villus in infected untreated mice versus all treated groups were of p-value < 0.001. Nonetheless, all therapeutic protocols were of p-value > 0.05 versus healthy control. Further details are in Table 3 and Figures 2 and 3.

Muscle phase of T. spiralis *infection (Day 35 p.i., chronic phase)*
The burden of T. spiralis larvae/LPF
The mean counts of *T. spiralis* larvae in the infected untreated mice were 21.2 ± 5.73 with a p-value < 0.001 compared to the treated and healthy study subgroups. In comparison, the IVM-treated subgroup showed mean counts of larvae/LPF of 6.8 ± 2.53 and a reduction percentage of 68 %. In ACV-treated subgroups, mean counts of larvae/LPF were 6.5 ± 2.22 with a reduction percentage of 69.34 %. The highest reduction percentage was found in the

	Subgroup 1B (infected untreated)		Subgroup 2B (IVM treated)		Subgroup 3B (ACV treated)		Subgroup 4B (combined treatment)		Subgroup 5B (healthy)		P-value
	M°	SD	M°	SD	M°	SD	M°	SD	M°	SD	
Larva burden/LPF	21.20[a]	5.73	6.80[b]	2.53	6.50[b]	2.22	2.70[b]	1.16	NA	.	< 0.001

NA – not applicable; in the superscripts – similar letters, p-value > 0.05, while different letters p-value < 0.05.

combined treatment (87.3 %) with mean counts of 2.7 ± 1.16. IVM and ACV-treated mice were of insignificant difference (p-value = 1). Likewise, both subgroups showed p-values of 0.06 and 0.09 when compared with the combined treatment Table 4.

Muscular histopathological changes

Significant differences were recorded between infected untreated mice (subgroup 1B) and treated subgroups (p-value < 0.001). Infected untreated mice showed the presence of intact larvae encompassing stichocyte, immature reproductive tract, lateral cord, intestinal tract, and the septum that separates the larvae from the nurse cell. In addition, the mature nurse cells showed eosinophilic cytoplasm and were surrounded by collagen capsules and intense inflammatory infiltrates. Notably, satellite cells under the basal lamina of the nurse cell and multiple nuclei invading the nurse cell cytoplasm were frequently present. The surrounding muscle fibers were atrophied in Fig. 4. Drug regimens altered the structure of the larvae and the nurse cells. Of note, IVM, not ACV-treated mu-

rine models, revealed scanty and relatively basophilic cytoplasm. Further details concerning histological parameters are shown in Table 5.

Immunohistochemistry
Expression of CDX2

In IVM-treated mice (Fig. 6E) and ACV-treated animals (Fig. 6F), the mean OD of CDX2 was 0.58 ± 0.1 and 0.63 ± 0.07 with p-values < 0.05 if compared with the infected untreated animals (subgroup 1A) (0.79 ± 0.1) (Fig. 6A-D). In the combined treatment (subgroup 4A), the mean OD of CDX2 was 0.34 ± 0.15 with p-values of < 0.001 when compared with subgroups 1A, 2A, and 3A. Nevertheless, subgroup 4A showed an insignificant difference when compared with the healthy control (p-value = 1).

Expression of Cyclin D1

Cyclin D1 was profoundly expressed in infected untreated animals (0.82 ± 0.08, p-value < 0.001). The IVM and ACV-treated
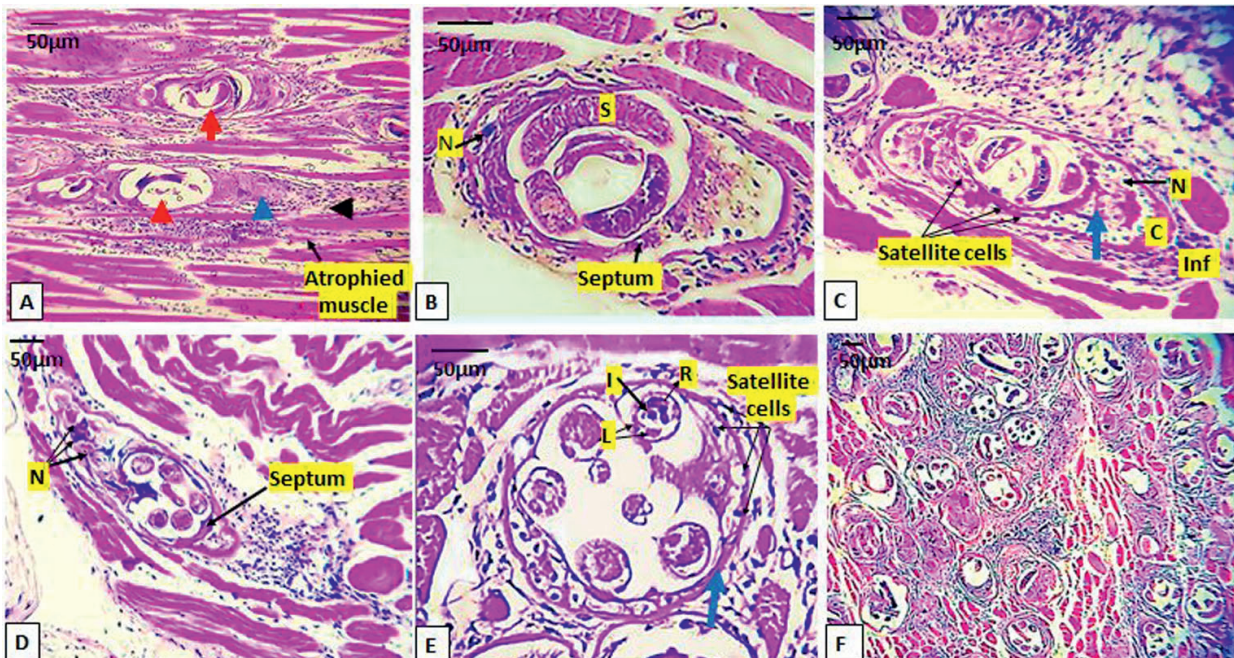
Fig. 4. Photomicrographs of H&E-stained muscle cut sections in infected untreated mice at day 35 p.i.. (A) Spiral morphology of larva (red arrow), nurse cell (blue arrow), capsule (black arrow), and atrophied muscle fibers. (B) The detailed structure of the encysted larva: stichocyte (S), hypertrophied nucleus (N). Note the septum that separates the parasite and nurse cell. (C) Mature nurse cells with eosinophilic non-homogeneous cytoplasm (blue arrow), collagen capsule (C) and intense inflammatory infiltrates (Inf), and satellite cells (under the basal lamina of the nurse cell) (D) hypertrophied nuclei (N) invading a nurse cell. (E) immature reproductive tract (R), lateral cord (L), intestinal tract (I), and blue arrow refers to nurse cell basal lamina (F) A cluster of larvae with intense inflammatory cells.

Table 5. Muscular histopathological changes on day 35 p.i. (chronic stage).

		Subgroup 1B (infected untreated)		Subgroup 2B (IVM treated)		Subgroup 3B (ACV treated)		Subgroup 4B (combined treatment)		Subgroup 5B (healthy)		P-value
		Count	%	Count	%	Count	%	Count	%	Count	%	
Larva structures	Intact	10[a]	100.0%	5[b]	50.0%	6[b]	60.0%	0[c]	0.0%	0	0.0%	< 0.001
	Altered	0[a]	0.0%	5[b]	50.0%	4[b]	40.0%	10[c]	100.0%	0	0.0%	
Capsule inflammatory infiltration	Mild	0[a]	0.0%	2[a,b]	20.0%	5[b,c]	50.0%	9[c]	90.0%	0	0.0%	< 0.001
	moderate	3[a,b]	30.0%	6[b]	60.0%	5[a,b]	50.0%	1[a]	10.0%	0	0.0%	
	intense	7[a]	70.0%	2[b]	20.0%	0[b]	0.0%	0[b]	0.0%	0	0.0%	
Nurse cell	intact	10[a]	100.0%	4[b]	40.0%	5[b]	50.0%	2[b]	20.0%	0	0.0%	0.001
	altered	0[a]	0.0%	6[b]	60.0%	5[b]	50.0%	8[b]	80.0%	0	0.0%	

In the superscripts, similar letters, p-value > 0.05 while different letters p-value < 0.05.

mice expressions were (0.52 ± 0.08 and 0.53 ± 0.09, p-value =1). In the combined treatment (subgroup 4B), Cyclin D1 showed OD (0.2 ± 0.07), and the healthy group showed insignificant differences (0.18 ± 0.06, p-value = 1), (Fig. 7).

Expression of CD 34
The lowest levels of CD34 expression (0.19 ± 0.07, p-value < 0.001) were present in the infected untreated mice (subgroup 1B). The mean OD of CD34 in IVM-treated mice and ACV-treated animals was 0.55 ± 0.11 and 0.43 ± 0.09, respectively, p-value = 0.098. Intense CD34-positive reactions were observed in the combined treatment (subgroup 4B) (0.75 ± 0.11, p-value = 1 versus healthy mice) with p-values < 0.001 when compared to subgroups 1B, 2B, and 3B, (Fig. 8).

Correlation of CDX2, Cyclin D1, and CD34 expressions with body weight, intestinal inflammation, and parasite burden
Overall, CDX2 in intestinal tissues (day 7 p.i.) positively correlated with the counts of lymphocytes, goblet cells, Paneth cells, crypts, and the adult and larva burden in tissue with p-values < 0.001.
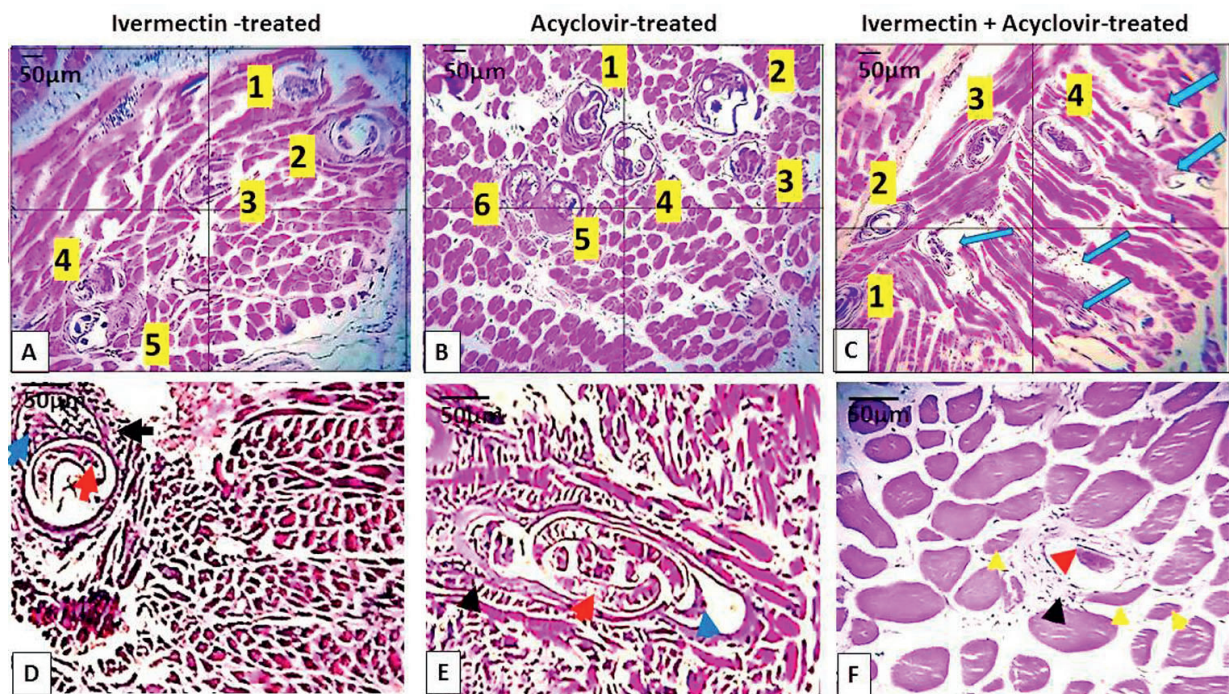
Fig. 5. Photomicrographs of H&E-stained muscle sections in infected and treated mice at day 35 p.i.. A, B, and C show the burden of larvae in treated groups. In D, the IVM-treated group showed nurse cells with scanty and slightly basophilic cytoplasm (blue arrow), moderate inflammatory infiltrates (black arrow), a remnant of larvae (red arrow), and atrophied unoccupied muscle fibers. In E, the ACV-treated group showed nurse cells with eosinophilic cytoplasm (blue arrow), mild to moderate inflammatory infiltrates (black arrow), variably damaged larvae (red arrows), and atrophied unoccupied muscle fibers. In (F) Combined treatment shows inflammatory infiltrates that partially invade the loose and vacuolated capsule (black arrow), homogenized larva lacking details (red arrow), regenerated muscle fibers (yellow arrows), and absence of muscle atrophy, while nurse cell was almost lacking.
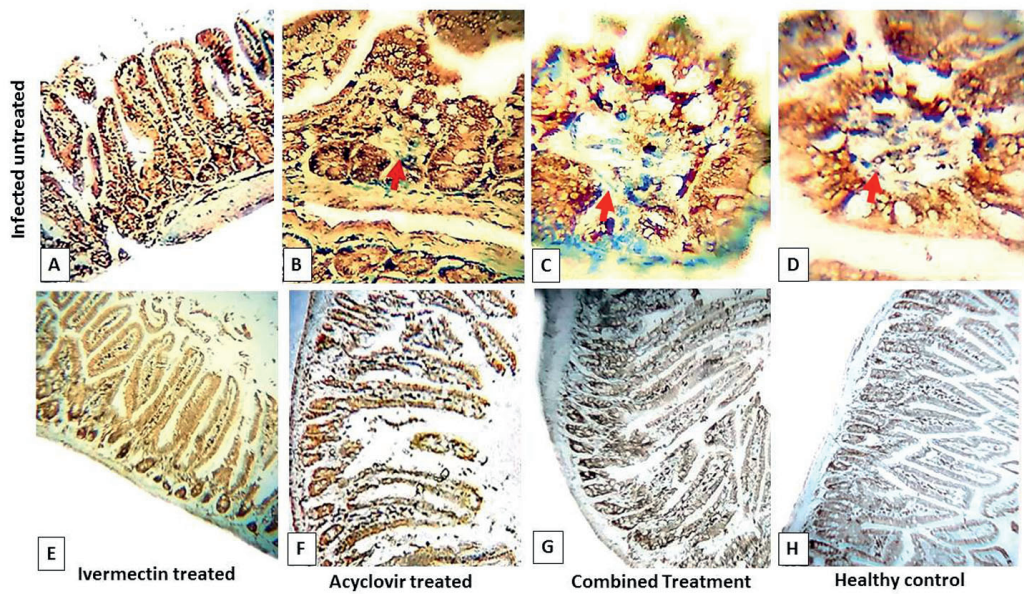
Fig. 6. Photomicrographs of immunohistochemical expression of CDX2 in the epithelial cells of the villi and crypts at day 7 p.i.. (A-D) Infected untreated mice show overexpression of nuclear and cytoplasmic CDX2. Note in (B-D) adult *T.spiralis* embedded in the villi (red arrows). E and F show reduced expression of CDX2 in IVM- and ACV-treated mice respectively. G, combined treatment shows mainly nuclear staining for CDX2. H, healthy control.
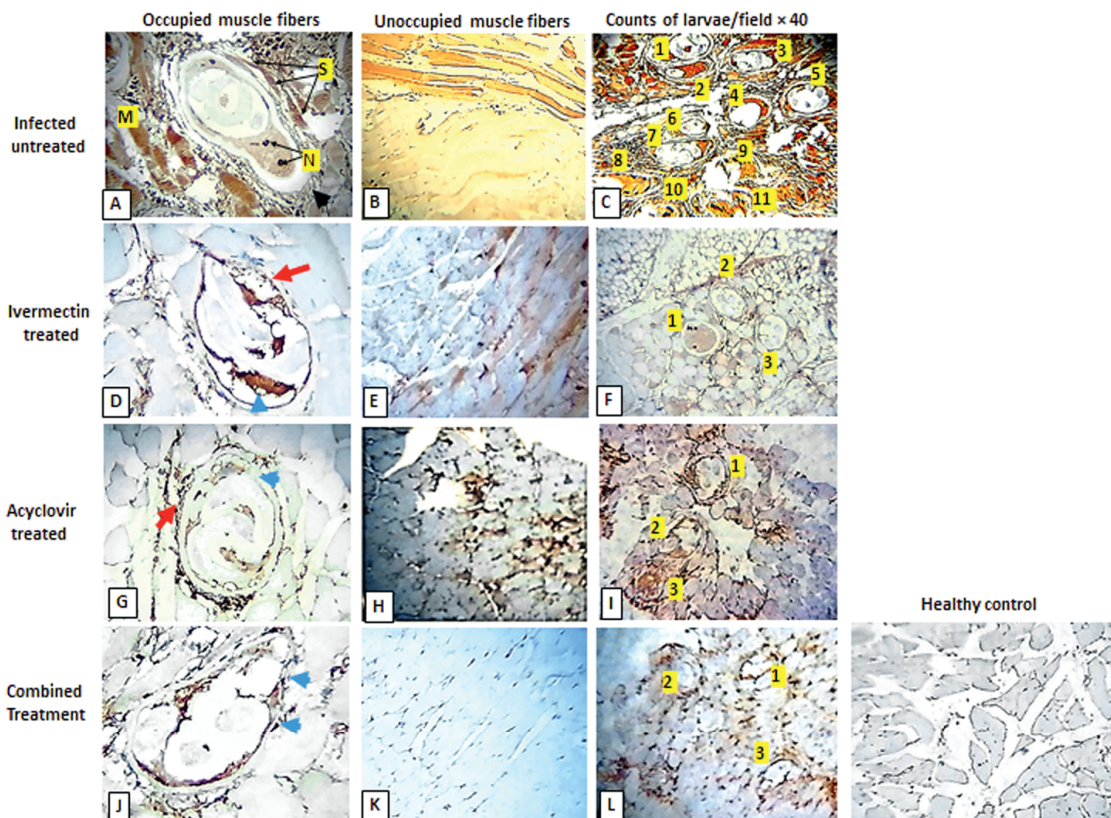
Fig. 7. Photomicrograph showing immunohistochemical expression of Cyclin D1 in the muscle phase (day 35 p.i.). A, Infected untreated animals show intense cytoplasmic and nuclear expression of Cyclin D1 in the nurse cell (N), satellite cells (S), and the surrounding muscle fibers (M). B and C show expression of CyclinD1 in unoccupied muscle fibers and clusters of encysted larvae respectively in infected untreated mice. Expression of Cyclin D1 declined in IVM (D-F) and ACV (G-I) treated groups in the capsules (red arrow), nurse cells (blue arrow), and unoccupied muscle fibers. J-L, combined treatment shows a profound reduction in CyclinD1 in both nurse cell remnants and unoccupied muscle fibers.

132

Occupied muscle fibers

Infected untreated (A)

Ivermectin treated (B)

Acyclovir treated (C)

Combined Treatment (D)
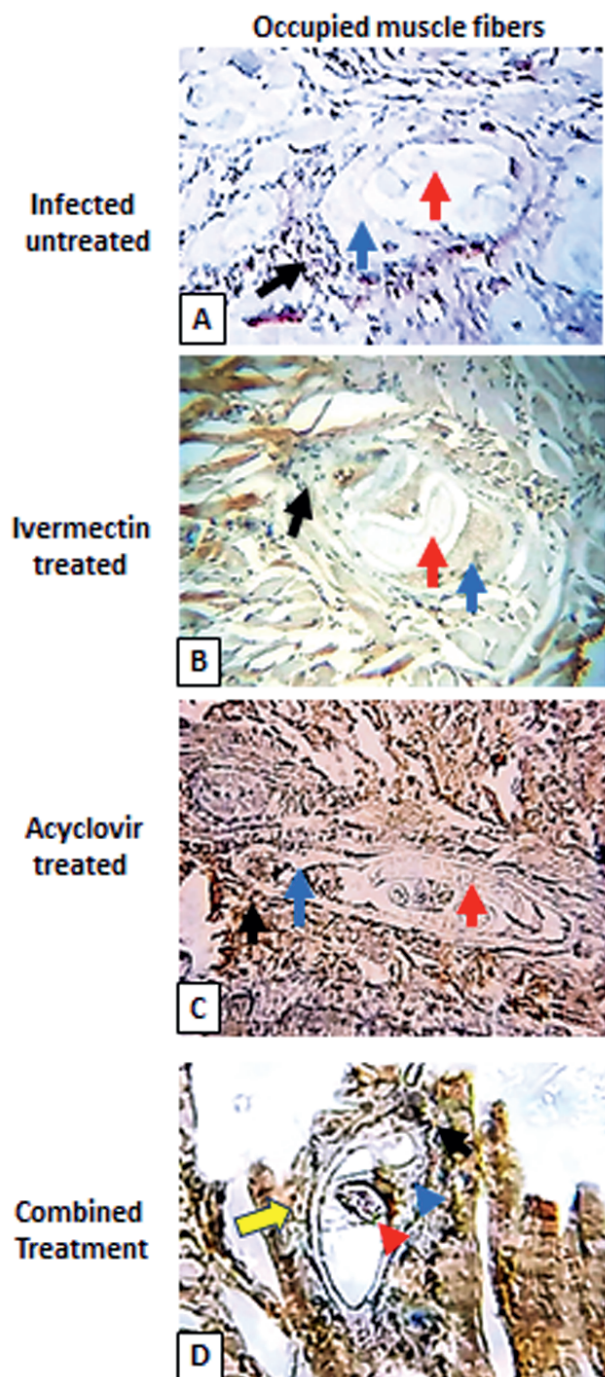
Fig. 8. Photomicrograph showing immunohistochemical expression of CD34 in the muscle phase (day 35 p.i.). (A) The infected untreated group shows missing or reduced CD34 localized between the individual muscle fibers. The black arrow refers to localized CD34 in mononuclear cells. The IVM-treated mice (B) and the ACV-treated group (C) show a moderate increase in the expression of CD34. (D) combined treatment shows intensification in the transmembrane expression of CD34 in association with remnants of nurse cells, damaged larva, and scarce cellular infiltrates. Note yellow arrow refers to immune reactive satellite cells. The black arrow refers to the capsule; the red arrow refers to the larva; and the blue block points to the remnants of the nurse cell.

Nonetheless, there were negative correlations between CDX2 in the intestine and the V length /C depth ratios (7-day p.i.) (r = -0.496, p-value < 0.001) and weight gain (days 7 and 35 p.i.) (r = -0.717 and -0.684 respectively, p-values < 0.001), (Fig. 9).

Likewise, Cyclin D1 in muscle tissue (day 35 p.i.) showed a negative correlation with V length /C depth ratios (day 7 p.i.) (r = -0.609, p-value < 0.001) and body weight (days 7 and 35 p.i.). (r = -0.853 and -0.829 respectively, p-value < 0.001). In contrast, other histological parameters in intestinal and parasite burden positively correlated (p-values < 0.001).

In contrast, the optical densities of CD34 in the muscles (day 35 p.i.) showed a positive correlation with V length /C depth ratios (day 7 p.i.) (r = 0.647, p-value < 0.001) and body weight (days 7 and 35 p.i.) (r = 0.727 and 0.746 respectively, p-value < 0.001). Yet, a negative correlation was present between the expression of the muscular CD34 and other intestinal parameters and parasite burden (p-value < 0.001), (Table 6).

Correlations between CDX2, Cyclin D1, and CD34 expressions
Intestinal CDX2 and muscular CyclinD1 correlated positively with an r-value of 0.847 (p-value < 0.001). Muscular CD34 and intestinal CDX2 were negatively correlated (r = -0.776, p-value < 0.001), and CD34 and Cyclin D1 in muscles were likewise negatively correlated (r = -0.883, p-value < 0.001), (Table 6).

Discussion

The present work showed an improved survival rate related to the three therapeutic lines of treatment (IVM, ACV, and combined treatment). IVM has been approved for the anti-helminthic therapy of onchocerciasis, strongyloidiasis, and filariasis (Nicolas *et al.*, 2020). Also, Michael *et al.* (2021) determined low mortality rates of sea lion pups treated with IVM. Oral IVM is extremely lipophilic and approaches "T-max" or the peak plasma concentration in 4 hours (Schmith *et al.*, 2020). In addition, IVM possesses an anti-inflammatory effect similar to dexamethasone (Khan *et al.*, 2023). Nevertheless, Schmith *et al.* (2020) speculated on the necessity of reassuring IVM as a management tool to avert possible anthelmintic resistance. Schuierer *et al.* (2020) determined that ACV treatment was related to meaningfully more prolonged survival in ICU patients. In addition, ACV is characterized by its extreme tolerability and safety in infants. It was deduced to be suitable for long-term systemic therapy (over a year), (Mavrutenkov *et al.*, 2019).

Infected untreated mice showed a significant reduction in body weight. *T. spiralis* has been related to loss of weight in the infected host as it shifts immunity toward macrophage (M2) proliferation, inhibits the pro-inflammatory reaction, and alters metabolism and the composition of enteric microbiota (Elsaftawy and Wassef, 2021; Sun *et al.*, 2024). Both the IVM and ACV regimens (subgroups 2 and 3) appeared to be efficient at preserving an acceptable body weight compared with infected untreated models. However, the evidence of combining the two regimens (IVM+ACV) (subgroup 4)
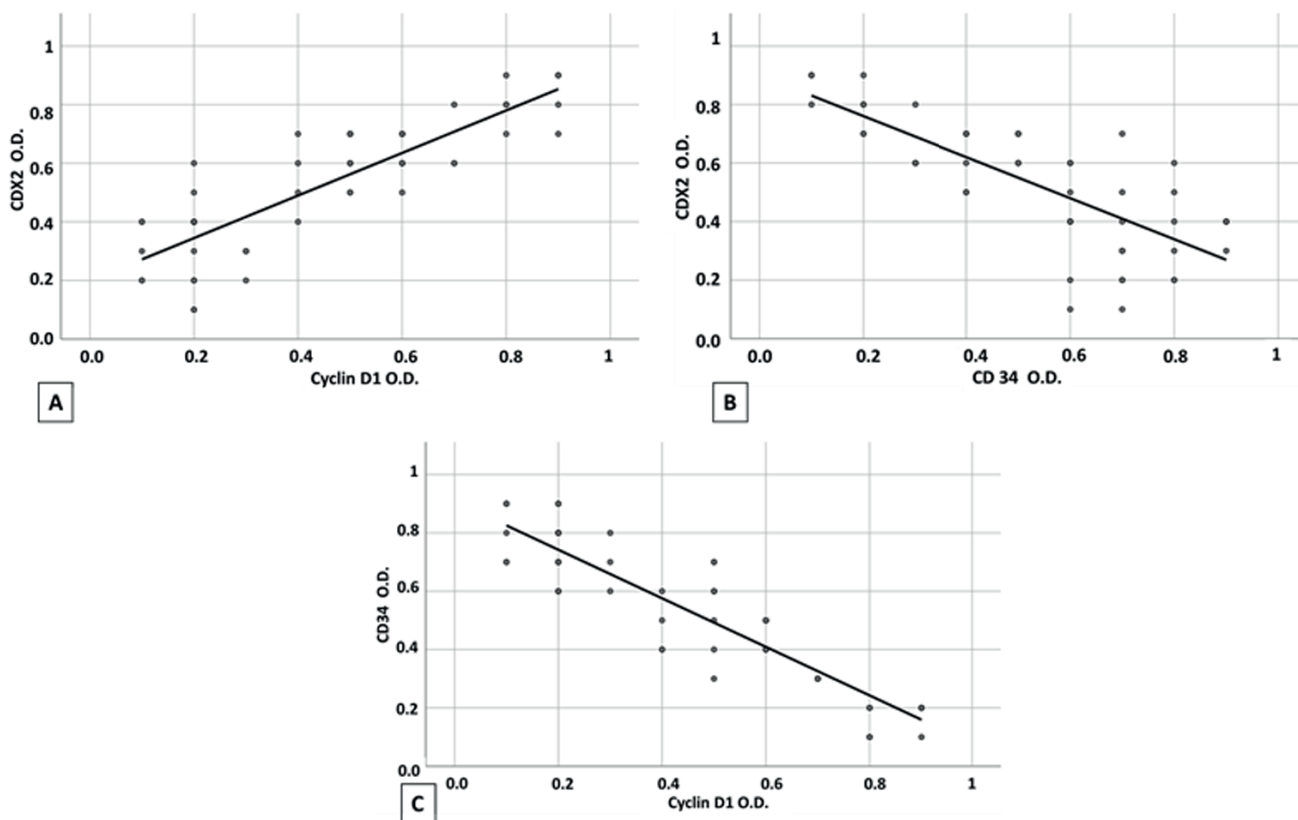
Fig. 9. Graphs of Spearman correlation. (A) Positive correlation between intestinal CDX2 O.D. (day 7 p.i.) and muscular Cyclin D1 expression (day 35 p.i.), (B) negative correlation between intestinal CDX2 (day 7 p.i.) and muscular CD34 (day 35 p.i.), and (C) negative correlation between muscular CD34 and Cyclin D1(day 35 p.i.).

body weight was analogous to healthy animals. Thus, combined treatment appeared to exert better anti-helminthic performance and chances of recovery (Rashid *et al*., 2022).

The combination administration of IVM and ACV monotherapies showed a significant reduction in the intestinal worm count per milliliter of enteric fluid and per 100 villi. Martin *et al*. (2021) speculated that IVM hinders the production of substances that suppress host immunity in filarial infections. IVM is an allosteric modulator that acts on the glutamate-gated chloride channels present in the nematodes (Martin *et al*., 2021). Regarding ACV, Benedetti *et al*. (2018) deduced its cytotoxic action in acute T-cell leukemia by inducing caspase-3 and nuclear DNA fragmentations. Thus, in the current model, adult counts were reduced despite the well-known immune escape action of helminthic infection. Pachnio *et al*., (2015) determined that ACV at low doses potentially enhances overall immune response. Of note, Ramakrishna *et al*. (2020) speculated that long-term ACV treatment hampers the functionality of the gut barrier and diminishes Bacteroidetes and Akkermansia muciniphila. Therefore, in the current study, short-term ACV therapy appeared to be a healing-promoting factor.

Overall, the three therapeutic regimens showed restored V length /C depth ratios. Sarkar *et al*. (2022) showed that in rotavirus-infect-

ed mice, IVM is efficient in restoring damaged intestinal villi, reducing the shedding of pathogen particles, and diminishing the expression of its protein. Also, Ristić *et al*. (2023) demonstrated that ACV was efficient in terminating mucous and bloody diarrhea and restoring functionality of intestinal villi through rectifying anemia, hypocalcemia, and hypokalemia in Varicella zoster virus infection. Estimation of lymphocyte counts from histologic sections showed an intense increase in infected untreated animals. Saracino *et al*. (2020) deduced that acute *T. spiralis* infection triggers intense inflammation and histological changes involving B and T lymphocytes with initial Th1 cytokine profile (IFN-γ and IL-12), then shift towards Th2 cytokine profile (increased levels of IL-4, IL-5, IL-13, Ig G1, and Ig E). Besides, the lamina propria cells exert "helmintho-toxic activity". Thus, the intestine converts to a site destructive to the migrant larvae, hindering their approach to the muscles. A significant reduction in villous lymphocytes was observed in all treated groups, wherein combined treatment scored the best records. Sadowski *et al*. (2014) deduced the capability of ACV to ameliorate duodenitis in Herpes simplex infections. Yao *et al*. (2013) showed the dramatic capability of ACV to trigger apoptosis of the tumor cells, particularly when enforced with nanoparticles. However, it remains questionable whether ACV can exert an apop-

Table 6. Correlation of CDX2, Cyclin D1, and CD34 expressions with body weight, intestinal inflammation, and parasite burden.

		CDX2	Cyclin D1	CD34
Body weight (g) at day 7 p.i.	Correlation Coefficient, r-value	-0.717-	-0.853-	0.727
	p-value	< 0.001	< 0.001	< 0.001
	No.	50	50	50
Body weight (g) at day 35 p.i.	Correlation Coefficient, r-value	-0.684-	-0.829-	0.746
	p-value	< 0.001	< 0.001	< 0.001
	No.	50	50	50
V length /C depth ratio	Correlation Coefficient, r-value	-0.496-	-0.609-	0.647
	p-value	< 0.001	< 0.001	< 0.001
	No.	50	50	50
lymphocyte counts/villus	Correlation Coefficient, r-value	0.759	0.896	-0.799-
	p-value	< 0.001	< 0.001	< 0.001
	No.	50	50	50
Goblet cell counts /villus	Correlation Coefficient, r-value	0.731	0.761	-0.718-
	p-value	< 0.001	< 0.001	< 0.001
	No.	50	50	50
No. of Paneth cells/crypt	Correlation Coefficient, r-value	0.550	0.645	-0.619-
	p-value	< 0.001	< 0.001	< 0.001
	No.	50	50	50
No. of crypts /villus	Correlation Coefficient, r-value	0.644	0.714	-0.685-
	p-value	< 0.001	< 0.001	< 0.001
	No.	50	50	50
Adult burden/milliliter at day 7 p.i.	Correlation Coefficient, r-value	0.783	0.834	-0.755-
	p-value	< 0.001	< 0.001	< 0.001
	No.	40	40	40
Adult burden/100 villi at day 7 p.i.	Correlation Coefficient, r-value	0.770	0.837	-0.736-
	p-value	< 0.001	< 0.001	< 0.001
	No.	40	40	40
larva burden/LPF at day 35 p.i.	Correlation Coefficient, r-value	0.690	0.799	-0.802-
	p-value	< 0.001	< 0.001	< 0.001
	No.	40	40	40

No., the number of mice, 50 mice in all parameters except in parasite burden was determined on 40 mice as healthy controls (10 mice) were not involved.

totic effect on inflammatory cells, thus ameliorating inflammation. Lee and Baldridge (2019) exhibited that by applying an antiviral cocktail involving ACV, intestinal lymphocytes revealed minor proliferation and more apoptosis than intestinal lymphocytes from untreated animals. This effect appeared to be highly specific to intestinal lymphocytes, whereas immune cells in other portions of the intestine, e.g., Peyer's patches and the lamina propria, remain unaffected. This was attributed to the disruption of the beneficial commensal viruses (not bacteria) by the antiviral treatment.
Regarding IVM, Yahia *et al*. (2022) showed that this drug reduces eosinophil counts and serum levels of IL-5. In addition, IVM was found to trigger apoptosis in a tumor model (Alghamdi *et al*., 2022), and in vitro, it showed suppressive activity on both DNA and RNA viruses (Banerjee *et al*., 2020). Hence, these speculations also explain the reductions in the lymphocytic counts.
Significant increases in the goblet and Paneth cells; crypt hyperplasia was a remarkable trait in the infected untreated animals. On the contrary, the three therapeutic protocols applied in this study significantly ameliorated these histological changes. Since early literature, the expulsion of adult worms appeared to be related to the histological repair of crypt hyperplasia and villus atrophy. Yet, the complete recovery is immune-dependent, and T cell depletion

in mice exhibits delayed recovery and atypical localization of the nematode (Manson-Smith *et al*., 1979; Saracino *et al*., 2020).

The muscle phase of infected untreated mice revealed the presence of whole and intact encapsulated larvae. The formation of nurse cells is complicated and involves molecular responses in the infected myocyte and satellite cells (Wu *et al*., 2008). Infected untreated mice predominantly revealed the eosinophilic cytoplasm of the nurse cells. Yet, IVM, not ACV-treated mice, showed scanty and relatively basophilic cytoplasm. Boonmars *et al*. (2004) showed that the eosinophilic cytoplasm of the nurse cell is of satellite cell origin, wherein the anti-apoptosis factor (PKB) predominates. Contrarywise, the basophilic cytoplasm is rich in the pro-apoptosis factors, Caspase-9, BAX, and Apaf-1, and originates from the infected myocyte.

Infected untreated mice showed capsule formation with intense inflammatory infiltrates that were reduced in IVM and ACV monotherapies and combined treatments. Beiting *et al*. (2004) determined that the capsule formation process initiates with small lymphocytic foci that increase progressively with macrophages. So far, eosinophils, dispersed plasma cells, and frequent lymphoblasts exist. Yet, these infiltrates invade the nurse cell, inducing focal necrosis. This may interpret the frequent appearance of nuclei we observed in the untreated nurse cells. We also noted septum, which is unique to *T. spiralis* and has been suggested to hinder the spread of damage in the whole length of the myocyte compared with another species, *T. pseudospiralis* (Wu *et al*., 2001). Exposure to the three therapeutic regimens damaged the internal details of the larvae together with the capsule inflammatory infiltrates and the nurse cell, whereas unoccupied muscle fibers were not atrophied. Yet, this might be attributed to their mode of action. IVM acts selectively on the pharyngeal muscles, the neurons, and the target glutamate-gated chloride channels of the nematodes while sparing the host. Also, IVM acts on the somatic muscle layer of the worm by antagonizing the nicotinic and (4)-aminobutyric acid (GABA) receptors (Abongwa *et al*., 2017). ACV hampers pathogens by inducing apoptosis-related genes and blocking the cell cycle, cellular replication, and activity of DNA polymerase enzyme (Liang *et al*., 2021).

In the intestinal phase, the immunohistochemical expression of epithelial CDX2 in infected untreated mice showed increased values that were positively correlated with parasite burden and inflammatory parameters in the intestine. Yet, the V length /C depth ratio and weight gain showed a negative correlation. Jahan *et al*. (2022) speculated that the CDX2 –TRIM31–NLRP3 signaling pathway triggers the expression of pro-inflammatory cytokines. Simultaneously, pro-inflammatory cytokines were also found to trigger either NF-κB or MAPK to stimulate the expression of CDX2 (Coskun *et al*., 2011). Increased intestinal CDX2 expression was related to early maturation of intestinal epithelium, disorganization of the crypt base, and alterations in the goblet and Paneth cell lines (Crissey *et al*., 2011). Also, mucin-2, the chief secretory mucin produced by goblet cells, is a CDX2 target (Mesquita *et al*., 2003).

CDX2 expression in mice treated with combination treatment (IVM+ACV) and the healthy control showed insignificant differences. Likewise, in COVID-19-related studies, ACV and IVM showed efficient anti-inflammatory effects (DiNicolantonio *et al*., 2020; Farasati Far *et al*., 2023). In addition, IVM promptly alleviated acetic acid-triggered colitis in rats (Aryannejad *et al*., 2022). However, the inhibitory effect exerted by IVM and/or ACV on CDX2 at a molecular level is a point of research. Noteworthy, successful treatment should not block but conserve the normal CDX2 expression levels, thus maintaining its repair functions and retaining the balanced renewal, proliferation, differentiation, and functionality of the epithelial cell lining (Coskun *et al*., 2011; Crissey *et al*., 2011). Also, adhesion genes, e.g., Claudin-2, are CDX2-targets, which are crucial to providing adhesion molecules for cell-cell interaction and hinder pathogen translocation (Sakaguchi *et al*., 2002). Chewchuk *et al*. (2021) deducted that loss of CDX function results in a definite reduction in the histocompatibility complex protein (H2-T3), decline in iCD8-α cell counts, intense infiltration of the macrophages and triggered pro-inflammatory reactions.

In the muscle phase, Cyclin D1 in infected untreated mice was over-expressed with a positive correlation to intestinal inflammation and parasite burden, negatively correlated with the V length /C depth ratio and body weight. Peer *et al*. (2008) deducted that Cyclin D1 is a potential anti-inflammatory protein that intensely upregulates in association with inflammation. In muscles, *T. spiralis* larvae appeared to subvert the differentiation of the infected myocyte by altering the cell cycle-related genes, hence blocking the cell cycle at the G2/M phase and transforming normal myocyte into a nurse cell (Bai *et al*., 2016), Qie and Diehl (2w016) related *T. spiralis* to the production of senescence factors and cell cycle inhibitors. In addition, Wu *et al*. (2006) deduced that trichinosis through c-Ski oncoprotein arrests the cell cycle and forms nurse cells in a TGF-β dependent pathway in the host cell's nucleus. Nevertheless, Qie and Diehl (2016) showed that cell cycle arrest in the nurse cell is a hyper-mitogenic G1-like type supported by increased expression of Cyclin-D1 and D2. In cancer cells, Wang *et al*. (2005) deduced that the excretory/secretory products of *T. spiralis* larvae induce the Ras signaling pathway that, in turn, upgrades the transcription of Cyclin D1 and constrains its proteolysis and extranuclear transfer (Alao, 2007). Of note, the overexpression of Cyclin D1 dysregulates cyclin-dependent kinase activity, accelerates cell growth under situations of restricted mitogenic pathways, evades chief cellular checkpoints, and eventually, carcinogenesis (Dabrowska *et al*., 2008; Latella *et al*., 2001). Therefore, pathology due to *T. spiralis* appeared to be related to the pathogenesis of cancer (Qie & Diehl, 2016).

Regarding ACV, a prior study showed that acute T-cell leukemia exerts cytotoxic action in Jurkat cells by inhibiting the cell cycle in the G1 and S phase phases and inducing cell apoptosis (Benedetti *et al*., 2018). Also, IVM was found to down-regulate cyclin D1 and arrest the cell cycle in the G0/G1 phase, thus inhibiting the proliferation of glioma cells and triggering cell apoptosis in vitro and in

vivo (Song *et al*., 2019).

The muscle phase also showed a reduction in the CD34 expression in the infected untreated mice with a negative correlation to intestinal inflammation and parasite burden and a positive relationship with ameliorated V length /C depth ratios and body weight. CD34 progenitor cells produce much more efficient and increased levels of Th2 cytokines than Th2 cells (Allakhverdi & Delespesse, 2012). Notably, the essential role of Type 2 immunity against the nematode is consequently necessary (Stear *et al*., 2023). Yet, Yong *et al*. (2002) determined that cell cycling and cellular division intimately affect the trans-endothelial migration of CD34 cell populations. CD34 cells were found to be enhanced in cells at the G0G1 phase and thus can efficiently migrate compared with those in the S/G2M phase. Also, cells in the S/G2M phase were found to be more adherent to the endothelial lining. Thus, their migration was reduced. Therefore, in the current model, whether this might be due to the extended inhibitory action of *T. spiralis* on the host cell cycle remains questionable. On the contrary, Mohammed *et al*. (2022) deduced that CD34 expression increases during the encapsulation of *T. spiralis* larvae owing to the associated myositis.

CD34 expression was ameliorated following treatment and, most notably, with the combined regimen. CD34 induces motility of satellite cells (progenitor cells) and their entrance into proliferation to enable competent regeneration of skeletal muscle (Alao, 2007). CD34 was also found to recover neovascularization (Ribatti, 2007). Other cellular functions involve the adhesion of lymphocytes to the walls of blood vessels and cell morphogenesis (Sidney *et al*., 2014). Ali *et al*. (2021) showed that ACV can efficiently trigger CD34 erythroid progenitors. A prior study showed that antiviral therapy normalizes CD34 cell functions (Dam Nielsen *et al*., 1998). Also, several studies revealed that IVM arrests the cell cycle at the G0/G1 phase (Juarez *et al*., 2020; Song *et al*., 2019), which, as we mentioned, is related to increased CD34 expression.

Intestinal CDX2 and muscular Cyclin D 1 exhibited a positive correlation. CDX2 in chronic gastritis was speculated to promptly induce intestinal metaplasia (Eda *et al*., 2002). Also, CDX2 has been related to cancer transformation and inflammatory bowel disease by disrupting innate immunity, tight junctions, and mucins (Crissey *et al*., 2011). Simultaneously, overexpression of Cyclin D1 is related to the early onset of cancer and the progression of tumors, as we have mentioned. Seriously, Cyclin D1 is related to the anchorage-independent survival and angiogenesis of tumors, while Fas expression becomes down-regulated, resulting in increased resistance to chemotherapies and hampered apoptosis (Shintani *et al*., 2002). Several studies considered the oncogenic capacity of *T. spiralis* that comes in association with immune modulation (Babal *et al*., 2011; Boros *et al*., 2019; Lichiardopol *et al*., 2010; Shirazi *et al*., 2015). In this context, *T.spiralis* might be regarded as a tumorigenic nematode.

Expressions of CD34 and Cyclin D1 in muscles were negatively correlated. Sadr *et al*. (2023) deduced that *T. spiralis* extracts arrest the cell cycle of solid tumors at the G1/S stage. This agreed with the increased Cyclin D1 expression recorded in the present study. Also, the reduced CD34 expression in *T. spiralis* infection has been related to hampered cellular migration, neovascularization, and tumor metastasis (Kang *et al*., 2013). Therefore, the concurrent Cyclin D1-CD34 inverse relationship made the oncogenic versus oncostatic effects of *T. spiralis* questionable.

Expression of muscular CD34 and intestinal CDX2 were negatively correlated. *T. spiralis* induces NF-κB in the macrophages (Guan *et al*., 2021), which stimulates the expression of CDX2 (Coskun *et al*., 2011). Nevertheless, adaptive Th2, regulatory T/B cells, the alternatively activated macrophages, and the inhibition of the DCs predominate the climate of the immune response (Ashour, 2013), irrespective of CDX2 (Wang *et al*., 2005). Therefore, in the current work, CDX2, despite showing increased intestinal expression, appeared inefficient in reducing the parasite load, and hence, CD34 expression in the muscle phase was subsequently affected and reduced.

Conclusion

Overall, the three therapeutic lines of treatment (IVM, ACV, and combined treatment) showed an improved survival rate and body weight compared with the infected untreated mice. The intestine of infected untreated mice showed higher counts of adult worms, lymphocytes, goblet cells, Paneth cells, and crypts, whereas the V length /C depth ratio recorded the lowest values. IVM and ACV monotherapies and combinations showed optimistic results regarding V length /C depth ratios and worm burden. Yet, lymphocyte counts were the only histopathological criteria that recorded lower counts in the ACV-treated groups (monotherapy and combined with IVM) compared with IVM-treated and infected untreated mice. The muscle phase of infected untreated mice revealed the definite criteria of encapsulated larvae. However, the combined treatment showed significant disruption of the encapsulated larvae and appeared to enhance muscle regeneration. The monotherapies achieved variable disruptive effects on the structure of the encapsulated larvae. In infected untreated mice, CDX2 and CyclinD1 showed a positive correlation with intestinal inflammation; nevertheless, CD34 revealed a negative correlation. CDX2 and CyclinD1 were positively correlated. CD34 was negatively correlated with CDX2 and CyclinD1. IVM +ACV significantly amended CDX2, CyclinD1, and CD34 expressions compared with monotherapies.

The current study paved the way for many perspectives, such as tumorigenicity versus the antitumor effects of *T. spiralis* infection on both intestinal and muscular tissues. Also, it remains to inquire if acyclovir can be used in all intracellular infections like *Toxoplasma*, *Leishmania*, and *Trypanosoma* infections. The therapeutic effects of acyclovir on parasites regarding Thymidine kinase and DNA breaks remain for study. Nevertheless, the applicability of acyclovir in parasitic infection is challenged due to other medical conditions, e.g., diabetes mellitus and tumors.

Conflict of Interest

The authors declare that there is no conflict of interest.

Availability of data and materials

All data and materials are available

References

ALLAKHVERDI, Z., DELESPESSE, G. (2012): Hematopoietic progenitor cells are innate Th2 cytokine-producing cells. *Allergy*, 67(1):4 – 9. DOI: 10.1111/j.1398-9995.2011.02703.x

ABONGWA, M., MARTIN, R.J., ROBERTSON, A.P. (2017): A brief review on the mode of action of antinematodal drugs. *Acta Vet (Beogr)*, 67(2): 137 – 152. DOI: 10.1515/acve-2017-0013

ALAO, J.P. (2007): The regulation of cyclin D1 degradation: roles in cancer development and the potential for therapeutic invention. *Mol Cancer*, 6: 24. DOI: 10.1186/1476-4598-6-24

ALFARO, L.A., DICK, S.A., SIEGEL, A.L., ANONUEVO, A.S., MCNAGNY, K.M., MEGENEY, L.A., CORNELISON, D.D., ROSSI, F.M. (2011): CD34 promotes satellite cell motility and entry into proliferation to facilitate efficient skeletal muscle regeneration. *Stem Cells*, 29(12): 2030 – 2041. DOI: 10.1002/stem.759

ALGHAMDI, H.A., AL-ZHARANI, M., ALJARBA, N.H., ALGHAMDI, A.A., AL-GHAMDI, A.A., ALDAHMASH, B.A., ELNAGAR, D.M., ALKAHTANI, S. (2022): Efficacy of ivermectin against colon cancer induced by dimethylhydrazine in male Wistar rats. *Saudi Pharm J*, 30(9): 1273 – 1282. DOI: 10.1016/j.jsps.2022.06.024

ALI, H., KHAN, F., GHULAM MUSHARRAF, S. (2021): Acyclovir induces fetal hemoglobin via downregulation of γ-globin repressors, BCL11A and SOX6 trans-acting factors. *Biochem Pharmacol*, 190: 114612. DOI: 10.1016/j.bcp.2021.114612

ARYANNEJAD, A., TABARY, M., NOROOZI, N., MASHINCHI, B., IRANSHAHI, S., TAVANGAR, S.M., MOHAMMAD JAFARI, R., RASHIDIAN, A., DEHPOUR, A.R. (2022): Anti-inflammatory Effects of Ivermectin in the Treatment of Acetic Acid-Induced Colitis in Rats: Involvement of GABA(B) Receptors. *Dig Dis Sci*, 67(8): 3672 – 3682. 10.1007/s10620-021-07258-x

ASHOUR, D. S. (2013): *Trichinella spiralis* immunomodulation: an interactive multifactorial process. *Expert Rev Clin Immunol*, 9(7): 669 – 675. DOI: 10.1586/1744666x.2013.811187

BABAL, P., MILCHEVA, R., PETKOVA, S., JANEGA, P., HURNIKOVA, Z. (2011): Apoptosis as the adaptation mechanism in survival of *Trichinella spiralis* in the host. *Parasitol Res*, 109(4): 997 – 1002. DOI: 10.1007/s00436-011-2343-2

BAI, X., HU, X., LIU, X., TANG, B., LIU, M. (2017): Current Research of Trichinellosis in China. *Front Microbiol*, 8: 1472. DOI: 10.3389/fmicb.2017.01472

BAI, X., WANG, X.L., TANG, B., SHI, H.N., BOIREAU, P., ROSENTHAL, B., WU, X.P., LIU, M.Y., LIU, X.L. (2016): The roles of supernatant of macrophage treated by excretory-secretory products from muscle larvae of *Trichinella spiralis* on the differentiation of C2C12 myoblasts. *Vet Parasitol*, 231: 83 – 91. DOI: 10.1016/j.vetpar.2016.07.033

BANERJEE, K., NANDY, M., DALAI, C.K., AHMED, S.N. (2020): The Battle against COVID 19 Pandemic: What we Need to Know Before we "Test Fire" Ivermectin. *Drug Res (Stuttg)*, 70(8): 337 – 340. DOI: 10.1055/a-1185-8913

BASYONI, M.M., EL-SABAA, A.A. (2013): Therapeutic potential of myrrh and ivermectin against experimental *Trichinella spiralis* infection in mice. *Korean J Parasitol*, 51(3): 297 – 304. DOI: 10.3347/kjp.2013.51.3.297

BEITING, D.P., BLISS, S.K., SCHLAFER, D.H., ROBERTS, V.L., APPLETON, J.A. (2004): Interleukin-10 limits local and body cavity inflammation during infection with muscle-stage *Trichinella spiralis*. *Infect Immun*, 72(6): 3129 – 3137. DOI: 10.1128/iai.72.6.3129-3137.2004

BEITING, D.P., PARK, P.W., APPLETON, J.A. (2006): Synthesis of syndecan-1 by skeletal muscle cells is an early response to infection with *Trichinella spiralis* but is not essential for nurse cell development. *Infect Immun*, 74(3): 1941 – 1943. DOI: 10.1128/iai.74.3.1941-1943.2006

BENEDETTI, S., CATALANI, S., PALMA, F., CANONICO, B., LUCHETTI, F., GALATI, R., PAPA, S., BATTISTELLI, S. (2018): Acyclovir induces cell cycle perturbation and apoptosis in Jurkat leukemia cells, and enhances chemotherapeutic drug cytotoxicity. *Life Sci*, 215: 80 – 85. DOI: 10.1016/j.lfs.2018.11.002

BOONMARS, T., WU, Z., NAGANO, I., TAKAHASHI, Y. (2004): Expression of apoptosis-related factors in muscles infected with *Trichinella spiralis*. *Parasitology*, 128(Pt 3): 323 – 332. DOI: 10.1017/s0031182003004530

BOROS, Z., GHERMAN, C.M., LEFKADITIS, M., COZMA, V. (2019): The oncogenic and oncostatic action of *Trichinella* spp. in animals. *Sci Parasitol*, 20(1-2): 5 – 11

CDC (2023): Trichinellosis. In *DPDx-Laboratory Identification of Parasites of Public health Concern*.

CHAN, Y.H. (2003a): Biostatistics 102: quantitative data--parametric & non-parametric tests. *Singapore Med J*, 44(8): 391 – 396

CHAN, Y.H. (2003b): Biostatistics 103: qualitative data - tests of independence. *Singapore Med J*, 44(10): 498 – 503

CHAN, Y.H. (2003c): Biostatistics 104: correlational analysis. *Singapore Med J*, 44(12): 614 – 619

CHEWCHUK, S., JAHAN, S., LOHNES, D. (2021): Cdx2 regulates immune cell infiltration in the intestine. *Sci Rep*, 11(1): 15841. DOI: 10.1038/s41598-021-95412-w

COSKUN, M., TROELSEN, J.T., NIELSEN, O.H. (2011): The role of CDX2 in intestinal homeostasis and inflammation. *Biochim Biophys Acta*, 1812(3): 283 – 289. DOI: 10.1016/j.bbadis.2010.11.008

CRISSEY, M.A., GUO, R.J., FUNAKOSHI, S., KONG, J., LIU, J., LYNCH, J.P. (2011): Cdx2 levels modulate intestinal ep.i.thelium maturity and Paneth cell development. *Gastroenterology*, 140(2): 517 – 528. e518. DOI: 10.1053/j.gastro.2010.11.033

DABROWSKA, M., SKONECZNY, M., ZIELIŃSKI, Z., RODE, W. (2008): Nurse cell of *Trichinella* spp. as a model of long-term cell cycle arrest. *Cell Cycle*, 7(14): 2167 – 2178. DOI: 10.4161/cc.7.14.6269

DAM NIELSEN, S., KJAER ERSBOLL, A., MATHIESEN, L., NIELSEN, J.O., HANSEN, J.E. (1998): Highly active antiretroviral therapy normalizes the function of progenitor cells in human immunodeficiency virus-infected patients. *J Infect Dis*, 178(5): 1299 – 1305. DOI: 10.1086/314464

DESPOMMIER, D.D. (1990): *Trichinella spiralis*: the worm that would be virus. *Parasitol Today*, 6(6): 193 – 196. DOI: 10.1016/0169-4758(90)90355-8

DESPOMMIER, D.D. (1998): How does *Trichinella spiralis* make itself at home? *Parasitol Today*, 14(8): 318 – 323. DOI: 10.1016/s0169-4758(98)01287-3

DINICOLANTONIO, J.J., BARROSO, J., MCCARTY, M. (2020): Ivermectin may be a clinically useful anti-inflammatory agent for late-stage COVID-19. *Open Heart*, 7(2): e001350. DOI: 10.1136/openhrt-2020-001350

DUBINSKÝ, P., ANTOLOVÁ, D., REITEROVÁ, K. (2016): Human Trichinella infection outbreaks in Slovakia, 1980 – 2008. *Acta Parasitol*, 61(2): 205 – 211. DOI: 10.1515/ap-2016-0029

EDA, A., OSAWA, H., YANAKA, I., SATOH, K., MUTOH, H., KIHIRA, K., SUGANO, K. (2002): Expression of homeobox gene CDX2 precedes that of CDX1 during the progression of intestinal metaplasia. *J Gastroenterol*, 37(2): 94 – 100. DOI: 10.1007/s005350200002

EL SAFTAWY, E.A., AMIN, N.M., SABRY, R.M., EL-ANWAR, N., SHASH, R.Y., ELSEBAIE, E.H., WASSEF, R.M. (2020): Can *Toxoplasma gondii* Pave the Road for Dementia? *J Parasitol Res*, 2020: 8859857. DOI: 10.1155/2020/8859857

ELSAFTAWY, E., WASSEF, R. (2021): Conceptions in parasite-microbiota relationships. *Parasitol. United J.*, 14(2): 133 – 140. DOI. 10.21608/puj.2021.69875.1113

FARASATI FAR, B., BOKOV, D., WIDJAJA, G., SETIA BUDI, H., KAMAL ABDELBASSET, W., JAVANSHIR, S., SEIF, F., PAZOKI-TOROUDI, H., DEY, S. K. (2023): Metronidazole, acyclovir and tetrahydrobiopterin may be promising to treat COVID-19 patients, through interaction with interleukin-12. *J Biomol Struct Dyn*, 41(10): 4253 – 4271. DOI: 10.1080/07391102.2022.2064917

FRANSSEN, F.F., FONVILLE, M., TAKUMI, K., VALLÉE, I., GRASSET, A., KOEDAM, M.A., WESTER, P.W., BOIREAU, P., VAN DER GIESSEN, J.W. (2011): Antibody response against *Trichinella spiralis* in experimentally infected rats is dose dependent. *Vet Res*, 42(1): 113. DOI: 10.1186/1297-9716-42-113

FREUND, J.N., DULUC, I., REIMUND, J.M., GROSS, I., DOMON-DELL, C. (2015): Extending the functions of the homeotic transcription factor Cdx2 in the digestive system through nontranscriptional activities. *World J Gastroenterol*, 21(5): 1436 – 1443. DOI: 10.3748/wjg.v21.i5.1436

FRISK, J.H., ERIKSSON, S., PEJLER, G., WANG, L. (2020): Identification of a novel thymidylate kinase activity. *Nucleosides Nucleotides Nucleic Acids*, 39(10-12): 1359 – 1368. DOI: 10.1080/15257770.2020.1755043

GAMBLE, H.R. (1996): Detection of trichinellosis in pigs by artificial digestion and enzyme immunoassay. *J Food Prot*, 59(3): 295 – 298. DOI: 10.4315/0362-028X-59.3.295

GOTTSTEIN, B., POZIO, E., NÖCKLER, K. (2009): Epidemiology, diagnosis, treatment, and control of trichinellosis. *Clin Microbiol Rev*, 22(1): 127 – 145, DOI: 10.1128/cmr.00026-08

GUAN, F., JIANG, W., BAI, Y., HOU, X., JIANG, C., ZHANG, C., JACQUES, M. L., LIU, W., LEI, J. (2021): Purinergic P2X7 Receptor Mediates the Elimination of *Trichinella spiralis* by Activating NF-κB/NLRP3/IL-1β Pathway in Macrophages. *Infect Immun*, 89(5): e00683-20. DOI: 10.1128/IAI.00683-20

HELAL, G., ASSER, L., ABDEL KADER, K.A., FADALI, G.A., ABDEL RAHMAN, Z.A. (1991): Immunohistochemical characterization of T-lymphocytes subsets in Egyptian hepatic schistosomiasis. *J Egypt Soc Parasitol*, 21(1): 195 – 202

JAHAN, S., AWAJA, N., HESS, B., HAJJAR, S., SAD, S., LOHNES, D. (2022): The transcription factor Cdx2 regulates inflammasome activity through expression of the NLRP3 suppressor TRIM31 to maintain intestinal homeostasis. *J Biol Chem*, 298(10): 102386. DOI: 10.1016/j.jbc.2022.102386

JUAREZ, M., SCHCOLNIK-CABRERA, A., DOMINGUEZ-GOMEZ, G., CHAVEZ-BLANCO, A., DIAZ-CHAVEZ, J., DUENAS-GONZALEZ, A. (2020): Antitumor effects of ivermectin at clinically feasible concentrations support its clinical development as a repositioned cancer drug. *Cancer Chemother Pharmacol*, 85(6): 1153 – 1163. DOI: 10.1007/s00280-020-04041-z

KANG, Y.J., JO, J.O., CHO, M.K., YU, H.S., LEEM, S.H., SONG, K.S., OCK, M.S., CHA, H.J. (2013): *Trichinella spiralis* infection reduces tumor growth and metastasis of B16-F10 melanoma cells. *Vet Parasitol*, 196(1-2): 106 – 113. DOI: 10.1016/j.vetpar.2013.02.021

KAPOOR, S., SHENOY, S.P., BOSE, B. (2020): CD34 cells in somatic, regenerative and cancer stem cells: Developmental biology, cell therapy, and omics big data perspective. *J Cell Biochem*, 121(5-6): 3058 – 3069. DOI: 10.1002/jcb.29571

KHAN, M.U.A., AKHTAR, T., NASEEM, N., AFTAB, U., HUSSAIN, S., SHAHZAD, M. (2023): Evaluation of therapeutic potential of ivermectin against complete Freund's adjuvant-induced arthritis in rats: Involvement of inflammatory mediators. *Fundam Clin Pharmacol*, 37(5): 971 – 982. DOI: 10.1111/fcp.12902

KONG, X., GUAN, J., MA, W., LI, Y., XING, B., YANG, Y., WANG, Y., GAO, J., WEI, J., YAO, Y., XU, Z., DOU, W., LIAN, W., SU, C., REN, Z., WANG, R. (2016): CD34 Over-Expression is Associated With Gliomas' Higher WHO Grade. *Medicine (Baltimore)*, 95(7): e2830. DOI: 10.1097/md.0000000000002830

LATELLA, L., SACCO, A., PAJALUNGA, D., TIAINEN, M., MACERA, D., D'ANGELO, M., FELICI, A., SACCHI, A., CRESCENZI, M. (2001): Reconstitution of cyclin D1-associated kinase activity drives terminally differentiated cells into the cell cycle. *Mol Cell Biol*, 21(16): 5631 – 5643.

DOI: 10.1128/mcb.21.16.5631-5643.2001

Lee, S., Baldridge, M. T. (2019): Viruses RIG up intestinal immunity. *Nat Immunol*, 20(12): 1563 – 1564. DOI: 10.1038/s41590-019-0530-y

Lefaan, Y.F.M., Hidayat, W., Nur'aeny, N. (2022): Tatalaksana infeksi herpes simpleks virus tipe-1 dan necrotizing ulcerative stomatitis pada anak dengan anemia aplastik Management of type-1 herpes simplex virus infection and necrotising ulcerative stomatitis in children with aplastic anaemia [Management of type-1 herpes simplex virus infection and necrotising ulcerative stomatitis in children with aplastic anaemia]. *J. Kedokt. Gigi Univ. Padjadjaran*, 33(3): 1 – 11. DOI: 10.24198/jkg.v33i3.30642 (In Indonesian)

Liang, C.S., Chen, C., Lin, Z.Y., Shen, J.L., Wang, T., Jiang, H.F., Wang, G.X. (2021): Acyclovir inhibits white spot syndrome virus replication in crayfish *Procambarus clarkii*. *Virus Res*, 305: 198570. DOI: 10.1016/j.virusres.2021.198570

Lichiardopol, C., Osman, I., Enache, S.D., Foarfă, C., Comănescu, V., Ghiluşi, M., Popescu, M. (2010): Thyroid regional metastasis from a giant cell malignant fibrous histiocytoma of the larynx in a patient with history of trichinellosis and tuberculosis. *Rom J Morphol Embryol*, 51(2): 359 – 363

Mademtzoglou, D., Relaix, F. (2022): From cyclins to CDKIs: Cell cycle regulation of skeletal muscle stem cell quiescence and activation. *Exp Cell Res*, 420(1): 113275. DOI: 10.1016/j.yexcr.2022.113275

Mañas-García, L., Guitart, M., Duran, X., Barreiro, E. (2020): Satellite Cells and Markers of Muscle Regeneration during Unloading and Reloading: Effects of Treatment with Resveratrol and Curcumin. *Nutrients*, 12(6): 1870. DOI: 10.3390/nu12061870

Manson-Smith, D.F., Bruce, R.G., Parrott, D.M. (1979): Villous atrophy and expulsion of intestinal *Trichinella spiralis* are mediated by T cells. *Cell Immunol*, 47(2): 285 – 292. DOI: 10.1016/0008-8749(79)90338-1

Martin, R.J., Robertson, A.P., Choudhary, S. (2021): Ivermectin: An Anthelmintic, an Insecticide, and Much More. *Trends Parasitol*, 37(1): 48 – 64. DOI: 10.1016/j.pt.2020.10.005

Mavrutenkov, V., Bolbot, Y., Shvaratska, O., Kazatska, O. (2019): The efficacy and safety of long-term systemic acyclovir therapy of neonatal herpes in immunocompetent children. *World Med. Biol.*, 67(1): 69 – 73. DOI: 10.26724/2079-8334-2019-1-67-69

Mesquita, P., Jonckheere, N., Almeida, R., Ducourouble, M.P., Serpa, J., Silva, E., Pigny, P., Silva, F.S., Reis, C., Silberg, D., Van Seuningen, I., David, L. (2003): Human MUC2 mucin gene is transcriptionally regulated by Cdx homeodomain proteins in gastrointestinal carcinoma cell lines. *J Biol Chem*, 278(51): 51549 – 51556. DOI: 10.1074/jbc.M309019200

Michael, S.A., Hayman, D.T.S., Gray, R., Roe, W.D. (2021): Risk Factors for New Zealand Sea Lion (*Phocarctos hookeri*) Pup Mortality: Ivermectin Improves Survival for Conservation Management. *Front. Mar. Sci.*, 8: 680678. DOI: 10.3389/fmars.2021.680678

Mohammed, H.S., Ghareeb, M.A., Aboushousha, T., Heikal, E.A. (2022): An appraisal of *Luffa aegyptiaca* extract and its isolated triterpenoidal saponins in *Trichinella spiralis* murine models. *Arab J Chem*, 15(11):104258. DOI: 10.1016/j.arabjc.2022.104258

Nicolas, P., Maia, M.F., Bassat, Q., Kobylinski, K.C., Monteiro, W., Rabinovich, N.R., Menéndez, C., Bardají, A., Chaccour, C. (2020): Safety of oral ivermectin during pregnancy: a systematic review and meta-analysis. *Lancet Glob Health*, 8(1): e92 – e100. DOI: 10.1016/s2214-109x(19)30453-x

Pachnio, A., Begum, J., Fox, A., Moss, P. (2015): Acyclovir Therapy Reduces the CD4+ T Cell Response against the Immunodominant pp65 Protein from Cytomegalovirus in Immune Competent Individuals. *PLoS One*, 10(4): e0125287. DOI: 10.1371/journal.pone.0125287

Pan, T.X., Huang, H.B., Lu, H.N., Zhao, G.X., Quan, Y., Li, J.Y., Xue, Y., Zhu, Z.Y., Wang, Y., Shi, C.W., Wang, N., Yang, G.L., Wang, C.F. (2023): NLRP3 Plays a Key Role in Antihelminth Immunity in the Enteral and Parenteral Stages of *Trichinella spiralis*-Infected Mice. *Infect Immun*, 91(4): e0038222. DOI: 10.1128/iai.00382-22

Peer, D., Park, E.J., Morishita, Y., Carman, C.V., Shimaoka, M. (2008): Systemic leukocyte-directed siRNA delivery revealing cyclin D1 as an anti-inflammatory target. *Science*, 319(5863): 627 – 630. DOI: 10.1126/science.1149859

Qie, S., Diehl, J.A. (2016): Cyclin D1, cancer progression, and opportunities in cancer treatment. *J Mol Med*, 94: 1313 – 1326. DOI: 10.4161/cc.7.14.6269

Quenelle, D.C., Birkmann, A., Goldner, T., Pfaff, T., Zimmermann, H., Bonsmann, S., Collins, D.J., Rice, T.L., Prichard, M.N. (2018): Efficacy of pritelivir and acyclovir in the treatment of herpes simplex virus infections in a mouse model of herpes simplex encephalitis. *Antiviral Res*, 149: 1 – 6. DOI: 10.1016/j.antiviral.2017.11.002

Ramakrishna, C., Mendonca, S., Ruegger, P.M., Kim, J.H., Borneman, J., Cantin, E.M. (2020): Herpes simplex virus infection, Acyclovir and IVIG treatment all independently cause gut dysbiosis. *PLoS One*, 15(8): e0237189. DOI: 10.1371/journal.pone.0237189

Rashid, M., Zahra, N., Chudhary, A., Rehman, T.U., Aleem, M.T., Alouffi, A., Mohammed, A., Rashid, M.I., Ehsan, M., Malik, M.I., Hussain Dilber, G., Bakhsh, A., Almutairi, M.M. (2022): Cost-benefit ratio of anthelmintic treatment and its comparative efficacy in commercial dairy farms. *Front Vet Sci*, 9(1047497. DOI: 10.3389/fvets.2022.1047497

Ribatti, D. (2007): The discovery of endothelial progenitor cells. An historical review. *Leuk Res*, 31(4): 439 – 444. DOI: 10.1016/j.leukres.2006.10.014

Ristić, A., Tamaš, O., Kovačević, M., Perović, B., Stanojević, M. (2023): Varicella zoster virus cerebral vasculopathy without rash accompanied by mucous and bloody diarrhea successfully treated with intravenous acyclovir: A case report. *J Clin Images Med Case Rep*, 4(3): 2307

Sadowski, B., Cirigliano, V., Betteridge, J. (2014): A Case of Asymptomatic Culture Positive Human Simplex Virus Duodenitis Treated with Acyclovir: 1116. *Am J Gastroenterol*, 109: S331

Sadr, S., Yousefsani, Z., Simab, P.A., Alizadeh, A.J.R., Lotfalizadeh, N., Borji, H. (2023): *Trichinella spiralis* as a potential antitumor

agent: An update. *World Vet J*, 13(1): 65 – 74. DOI: 10.54203/ scil.2023.wvj7

SAKAGUCHI, T., GU, X., GOLDEN, H.M., SUH, E., RHOADS, D.B., REINECKER, H.C. (2002): Cloning of the human claudin-2 5'-flanking region revealed a TATA-less promoter with conserved binding sites in mouse and human for caudal-related homeodomain proteins and hepatocyte nuclear factor-1alpha. *J Biol Chem*, 277(24): 21361 – 21370. DOI: 10.1074/jbc.M110261200

SARACINO, M.P., VILA, C.C., COHEN, M., GENTILINI, M.V., FALDUTO, G.H., CALCAGNO, M.A., ROUX, E., VENTURIELLO, S.M., MALCHIODI, E.L. (2020): Cellular and molecular changes and immune response in the intestinal mucosa during *Trichinella spiralis* early infection in rats. *Parasit Vectors*, 13(1): 505. DOI: 10.1186/s13071-020-04377-8

SARKAR, R., BANERJEE, S., HALDER, P., KOLEY, H., KOMOTO, S., CHAWLA-SARKAR, M. (2022): Suppression of classical nuclear import pathway by importazole and ivermectin inhibits rotavirus replication. *J Antimicrob Chemother*, 77(12): 3443 – 3455. DOI: 10.1093/ jac/dkac339

SCHALKWIJK, H.H., SNOECK, R., ANDREI, G. (2022): Acyclovir resistance in herpes simplex viruses: Prevalence and therapeutic alternatives. *Biochem Pharmacol*, 206: 115322. DOI: 10.1016/j. bcp.2022.115322

SCHMITH, V.D., ZHOU, J.J., LOHMER, L.R.L. (2020): The Approved Dose of Ivermectin Alone is not the Ideal Dose for the Treatment of COVID-19. *Clin Pharmacol Ther*, 108(4): 762 – 765. DOI: 10.1002/ cpt.1889

SCHUIERER, L., GEBHARD, M., RUF, H.G., JASCHINSKI, U., BERGHAUS, T. M., WITTMANN, M., BRAUN, G., BUSCH, D.H., HOFFMANN, R. (2020): Impact of acyclovir use on survival of patients with ventilator-associated pneumonia and high load herpes simplex virus replication. *Crit Care*, 24(1): 12. DOI: 10.1186/s13054-019-2701-5

SHINTANI, M., OKAZAKI, A., MASUDA, T., KAWADA, M., ISHIZUKA, M., DOKI, Y., WEINSTEIN, I.B., IMOTO, M. (2002): Overexpression of cyclin DI contributes to malignant properties of esophageal tumor cells by increasing VEGF production and decreasing Fas expression. *Anticancer Res*, 22(2a): 639 – 647

SHIRAZI, N., BIST, S.S., AHMAD, S., HARSH, M. (2015): *Trichinella spiralis*: Mere Co-Existence or Carcinogenic Parasite For Oral Squamous Cell Carcinoma? *J Clin Diagn Res*, 9(10): ED03 – ED04. DOI: 10.7860/jcdr/2015/14050.6585

SIDNEY, L.E., BRANCH, M.J., DUNPHY, S.E., DUA, H.S., HOPKINSON, A. (2014): Concise review: evidence for CD34 as a common marker for diverse progenitors. *Stem Cells*, 32(6): 1380 – 1389. DOI: 10.1002/stem.1661

SIRIYASATIEN, P., YINGYOURD, P., NUCHPRAYOON, S. (2003): Efficacy of albendazole against early and late stage of *Trichinella spiralis* infection in mice. *J Med Assoc Thai*, 86 Suppl 2: S257 – 262

SONG, D., LIANG, H., QU, B., LI, Y., LIU, J., ZHANG, Y., LI, L., HU, L., ZHANG, X., GAO, A. (2019): Ivermectin inhibits the growth of glioma cells by inducing cell cycle arrest and apoptosis in vitro and in vivo. *J Cell Biochem*, 120(1): 622 – 633. DOI: 10.1002/jcb.27420

STEAR, M., PRESTON, S., PIEDRAFITA, D., DONSKOW-ŁYSONIEWSKA, K. (2023): The Immune Response to Nematode Infection. *Int J Mol Sci*, 24(3): 2283. DOI: 10.3390/ijms24032283

SUN, X.M., HAO, C.Y., WU, A.Q., LUO, Z.N., EL-ASHRAM, S., ALOUFFI, A., GU, Y., LIU, S., HUANG, J.J., ZHU, X P. (2024): *Trichinella spiralis* -induced immunomodulation signatures on gut microbiota and metabolic pathways in mice. *PLoS Pathog*, 20(1): e1011893. DOI: 10.1371/journal.ppat.1011893

WANG, M.L., SHIN, M.E., KNIGHT, P.A., ARTIS, D., SILBERG, D.G., SUH, E., WU, G.D. (2005): Regulation of RELM/FIZZ isoform expression by Cdx2 in response to innate and adaptive immune stimulation in the intestine. *Am J Physiol Gastrointest Liver Physiol*, 288(5): G1074 – 1083. DOI: 10.1152/ajpgi.00442.2004

WIŃSKA, P., GOŁOS, B., CIEŚLA, J., ZIELIŃSKI, Z., FRACZYK, T., WAŁAJTYS-RODE, E., RODE, W. (2005): Developmental arrest in *Caenorhabditis elegans* dauer larvae causes high expression of enzymes involved in thymidylate biosynthesis, similar to that found in *Trichinella* muscle larvae. *Parasitology*, 131(Pt 2): 247 – 254. DOI: 10.1017/s0031182005007274

WOLCOTT, K.M., WOODARD, G.E. (2020): CD34 positive cells isolated from traumatized human skeletal muscle require the CD34 protein for multi-potential differentiation. *Cell Signal*, 74: 109711. DOI: 10.1016/j.cellsig.2020.109711

WU, Z., MATSUO, A., NAKADA, T., NAGANO, I., TAKAHASHI, Y. (2001): Different response of satellite cells in the kinetics of myogenic regulatory factors and ultrastructural pathology after *Trichinella spiralis* and *T. pseudospiralis* infection. *Parasitology*, 123(Pt 1): 85 – 94. DOI: 10.1017/s0031182001007958

WU, Z., NAGANO, I., BOONMARS, T., TAKAHASHI, Y. (2006): Involvement of the c-Ski oncoprotein in cell cycle arrest and transformation during nurse cell formation after *Trichinella spiralis* infection. *Int J Parasitol*, 36(10-11): 1159 – 1166. DOI: 10.1016/j.ijpara.2006.05.012

WU, Z., SOFRONIC-MILOSAVLJEVIC, L., NAGANO, I., TAKAHASHI, Y. (2008): *Trichinella spiralis*: nurse cell formation with emphasis on analogy to muscle cell repair. *Parasit Vectors*, 1(1): 27. DOI: 10.1186/1756-3305-1-27

YAHIA, S., AHMED, A., ALSHAFEY, M., MOAWAD, H. (2022): Comparing the anti-parasitic effect of Ivermectin versus Albendazole against intestinal nematode worms. *Parasitol. United J.*, 15(2): 165 – 173. DOI: 10.21608/puj.2022.143664.1172

YAO, J., ZHANG, Y., RAMISHETTI, S., WANG, Y., HUANG, L. (2013): Turning an antiviral into an anticancer drug: nanoparticle delivery of acyclovir monophosphate. *J Control Release*, 170(3): 414 – 420. DOI: 10.1016/j.jconrel.2013.06.009

YONG, K.L., FAHEY, A., PIZZEY, A., LINCH, D.C. (2002): Influence of cell cycling and cell division on transendothelial migration of CD34+ cells. *Br J Haematol*, 119(2): 500 – 509. DOI: 10.1046/j.1365-2141.2002.03837.x